

## **Author response to referee comments for the manuscript titled “Multi-Satellite Retrieval of SSA using OMI-MODIS algorithm”**

We thank both the referees for their valuable comments and suggestions in improving this manuscript. Please note that author comments (AC) are in red font color. The entire analysis has been redone using the latest version of OMI (v1.8.9). The modified manuscript along with the author marked changes are provided after the authors' response.

### **Anonymous Referee #1**

Here are my line-by-line comments. The most important is indicated by \*\*\*\*\*.

RC: Line 30. “Forcing” or “effect”. Some people use forcing only when the aerosols are anthropogenic. Clarification in the definition is needed here. IPCC reference to ‘forcing’ is only anthropogenic and that is where that statement is leading later on in the paragraph.

*AC: While the aerosol forcing definition according to IPCC is due to only anthropogenic aerosols, for the present study it is defined as the combined effect of both natural and anthropogenic aerosols.*

RC: Line 40-41. ‘the fraction of the total extinction of radiation attributed to scattering’

*AC: The statement has been modified accordingly.*

RC: Line 44-45. “However, SSA values lack high certainty (Bond and Bergstrom, 2006; Bond et al., 2013)” What has high uncertainty? Measurements of SSA? Attributing SSA to different aerosol types? Understanding the overall SSA of aerosols globally or regionally? “SSA values” is too ambiguous.

*AC: The sentence has been corrected as measurements of SSA.*

RC: Line 44-51. Lots of ambiguities here between measurements, retrievals and physical properties.

*AC: We thank the reviewer for pointing out the mistake. The phrase used is SSA retrievals.*

RC: Lines 52-72. \*\*\*\*\*While Table 1 is very good and a major contribution of the paper by itself. This paragraph needs clarification between “direct” and “indirect” measures of SSA. Again, what is a measurement? What is a retrieval? What are the pluses and minuses of each? I see that in the next paragraph some of this explanation is attempted, but the organization of the whole delivery is confusing. \*\*\*\*\*

*AC: We thank the reviewer for pointing out the mistake. The words 'direct' and 'indirect' are removed. The statement has been modified as follows "Studies on the various measurements of aerosol absorption using instruments and their uncertainty evaluation have been performed previously (Horvath, 1993, Heintzenberg et al., 1997; Moosmuller et al., 2009).*

*Along with ground-based retrievals of SSA, there have been other methods to retrieve the parameter using satellites (Table 1). The different methods of retrieval of SSA, both ground-based and using satellites, are provided in Table 1. Unlike aerosol absorption coefficient, SSA is not measured directly by an instrument. Instead, it is retrieved using lookup tables or estimated using other parameters which are measured or calculated using models."*

RC: Figure 1 caption. State the wavelength.

*AC: The wavelength has been added.*

RC: Line 214-215. Some places on the globe will not have a lot of retrievals because AOD is usually low and there is an AI criterion as to when to retrieve. There might only be one retrieval in that grid box in 5 years. Do the plots in Fig. 1 show points like these? Is that a fair representation of the climatology?

*AC: Yes, there are grid boxes which have only one retrieval in 5 years. Such boxes are not preferred as a climatological representation. If these boxes were removed, the number of points reduced drastically. However, Fig.1 is not considered as a climatology plot since it involves only five years of data. It is plotted to understand the spatial coverage and variation of both the algorithms for the different seasons over the five years. For better representation of climatology data over more years are required.*

RC: Lines 217-219. Are these statements based on Figure 1 or some previous work or understanding? Because they don't match what I see in Figure 1. Even if you ignore the tropical Atlantic because of dust, I see a lot of SSA in the 0.9 to 0.95 range in the open oceans and near land, I don't see anything that gets lower than 0.85. Where is the 0.75?

*AC: A narrower colour scale from 0.85 to 1 has been used to represent global SSA maps.*

RC: Line 220-221. From my own studies based on AOD<sub>550</sub>, not AI, the threshold is AOD<sub>550</sub> = 0.30. Greater than that and I don't see the ocean anymore.

*AC: We agree with the referee that over oceans AOD does not exceed 0.3 but we are talking about AI, not AOD*

RC: Lines 238-240. What happens when one method has a value and the other method does not? This should be stated in the text, and possibly the caption to Figure 2. This in itself is of a lot of interest to people. \*\*\*\*\*Why is OMI retrieving so much more than OMI-MODIS?\*\*\*\*\* You mention OMI is cloud contaminated and MODIS is not. Is this difference in the number of retrievals due to cloud masking? Can you prove that?\*\*\*\*\*Because the cloud masking issue is never addressed anywhere in the paper.\*\*\*\*\*

*AC: In the OMI-MODIS algorithm, the aerosol layer height was retrieved through linear interpolation of  $AOD_{OMI}$  at five different heights and  $AOD_{388}$  as a reference. Linear interpolation was not performed for OMI retrievals which had a missing value at any particular height or if the OMI retrieval was the same at all heights, resulting in the final OMI-MODIS value to be invalid. Similarly, if the MODIS AOD was found to be missing or invalid, the corresponding OMI-MODIS retrieval was also considered invalid. The removal of such invalid retrievals resulted in a reduction in the total number of valid points in OMI-MODIS algorithm when compared to OMI algorithm (Fig. 1b).*

*Gassó and Torres (2016) for a particular day over the North Central Atlantic compared the AOD values retrieved by OMI and MODIS. They compared the difference with the aerosol cloud mask retrieved by MODIS. It was found that while most of the retrievals of OMI screened the cloudy pixels, some of the best quality (flag=0) pixels were found to be cloud contaminated. They attributed this to the coarser pixel size of OMI compared to the smaller pixel size of MODIS cloud product. Using the MODIS cloud fraction to screen out OMI cloudy pixels improved the agreement between AOD values but resulted in a reduction in the number of OMI retrievals despite good agreement between the AOD values. In some cases, MODIS showed large cloud fraction values when the aerosol index was high implying the presence of aerosols above clouds. Hence Gassó and Torres concluded that only MODIS cloud fraction could not be used to screen out OMI pixels. Such an analysis is needed on a larger spatiotemporal scale which is beyond the scope of this manuscript and will be considered in a separate work.*

RC: Figure 2 caption. We need the wavelength of the SSA, and in the caption, it should tell us that it is OMI-MODIS minus OMI. It should also tell us what happens when one product has values and the other does not.

*AC: The wavelength has been added. When the OMI-MODIS SSA value was found invalid, the difference was also considered to be invalid.*

RC: Line 245-247. What are natural aerosols here and what are anthropogenic? Dust and smoke? Please clarify. Also, at least at this point it's not easy for me to see how differences in the method results are linked to actual aerosol properties. The speculation here seems premature. Most importantly, rather than dwelling on the differences in aerosol types/properties the text should mention problems with the height assumption. That would be my first guess as to what I'm seeing here, not aerosol types. Also the differences are relatively small, within what I would expect to be the uncertainty in any satellite retrieval of SSA.

*AC: As suggested by the reviewer the statement has been modified as follows "This was attributed to the change in aerosol layer height and (or) aerosol physical and optical properties." The different aerosol sources during different seasons were studied through trajectory analysis to understand the role of aerosol type in the change of SSA between algorithms. Following this discussion, the role of aerosol layer height in SSA retrieval was examined. The study by Torres et al. (2018) on the latest version of OMI aerosol product shows that the shape of dust aerosols assumed also affected the SSA retrievals implying the importance of knowing the aerosol type along with its physical properties for the retrieval of SSA.*

RC: Figure 4. That isn't southern Africa. Maybe call it Central Africa? Same for Figure 5.

*AC: The trajectory analysis for the Atlantic Ocean has been removed since it was found that the difference of SSA retrievals between the two algorithms over this region was within  $\pm 0.03$ .*

RC: Table 2 and 3. Don't use numbers for regions. Use their names. Also, this is not for the "Atlantic Ocean", but for one specific point in the Atlantic Ocean. Likewise, for the Arabian Sea.

*AC: The numbers are used only on the plot for ease in reading. The regions representing the numbers are mentioned in the caption as well as in the text. As suggested by the reviewer, the trajectory analysis was indicated for one specific point.*

RC: Lines 286-291. "Harriss et al. (1984), found that there is advection of anthropogenic pollutants from North America to the North Atlantic Ocean." I don't have time to look up that reference, but does it include that one point at 15N 45 W? Also 1984 is a long, long time ago. Aerosols in North America have changed significantly since then and your study period

is 2009-2010. Also there is no reference on the NOAA-11 study. 1988-2004. That's a bit better in terms of matching this paper's study period, but not much.

*AC: Since the difference in SSA between the algorithms was within the  $\pm 0.03$  range over the Atlantic Ocean, the trajectory analysis was done only for a point over the Arabian Sea and the Bay of Bengal to understand the aerosol sources that affect the region during each season and the variation of difference in SSA for each season.*

RC: Lines 299-300. I can visualize, maybe, a large-scale circulation that is creating westerlies aloft during winter and spring at that point. It would have to be the wintertime baroclinic systems dipping far south. The question though is that at least in winter there would be no aerosol associated with that flow. Springtime you may be getting biomass burning from Mexico. \*\*\*\*It would be useful to better describe the meteorology affecting the situation. \*\*\*\*\*

*AC: The trajectory analysis for the Atlantic Ocean has been removed.*

RC: Lines 302-331. The meteorological description here is much better than that over the Atlantic. Here, a single point in the middle of the Arabian Sea is better representative of the entire region than a single point in the north tropical Atlantic trying to represent the entire "Atlantic Ocean". But also the authors just convey a much clearer understanding of the meteorological and aerosol forces influencing that point in the Arabian sea than they do in the north tropical Atlantic.

*AC: We thank the reviewer for the comment.*

RC: Lines 332 -336. These sentences are so convoluted I don't understand the point the authors are trying to make.

*AC: The statement has been modified as follows "While the Arabian Sea is dominated by dust and oceanic aerosols, studies have shown that the Bay of Bengal is influenced by various air masses associated with Asian monsoon system including those of anthropogenic origin."*

RC: Lines 355-357. Here the terms natural and anthropogenic are being used without really defining them. \*\*\*\*Trajectory analysis overall. I don't see how all this work connects to the rest of the paper. \*\*\*\*

*AC: It has been previously mentioned that "The IGP with its heavy population and a large number of industries acts as a source for anthropogenic aerosols which are transported to*

*the Bay of Bengal during winter”. These along with the biomass aerosols are considered anthropogenic, and the sea-salt aerosols from nearby ocean and the dust from Arabian Peninsula and Indian subcontinent are considered natural aerosols. The trajectory analysis was performed to understand the seasonal variation of SSA of both the algorithms due to the difference in aerosol sources between seasons.*

RC: Lines 362-365. From the histograms I don't see much differences between the Atlantic and the Arabian Sea in terms of how well the results from the two methods match. What is considered “reasonably good agreement”?

*AC: The results mentioned are figures from Satheesh et al. (2009). In their study, they have compared MODIS extrapolated UV AOD with OMI AOD over the Atlantic Ocean and the Arabian Sea. They found that over the Atlantic on an average the AOD agreed within  $\pm 0.1$ . Over the Arabian Sea, they found agreement between both the AOD retrievals during the months when a large amount of dust aerosols is present (April-July).*

RC: Line 363. Can you remind the reader which season is the dust season? From the histograms, it looks like MAM is the least biased season, and that is not the dust season, right?

*AC: The dust season over the Arabian Sea is March-April-May. According to Satheesh et al. (2009), MODIS UV AOD and OMI AOD agreed well during this season when there is the large loading of dust.*

RC: Line 365, but I do agree that height should be the important factor, not aerosol type.

*AC: We agree with the reviewer that aerosol height is the main factor affecting the retrievals.*

RC: Lines 367-369. I'm not sure what is meant here. In this work the ALH is calculated for OMI using the best estimate of SSA retrieved from OMI. This is the operational OMI only retrieval we are talking about, not the OMI-MODIS retrieval, right? How is the best estimate SSA determined? This retrieval returns 5 ordered pairs of (SSA, ALH) and the retrieval fixes ALH and returns SSA. Fine. Now, in this work, the authors are going to fix SSA and return ALH. Ok. But: : : how do they decide on an SSA? The caption for Figure 7 explains it, but the text should match.

*AC: The OMI retrieval has been explained in section 2.1. Along with the aerosol products retrieved at different heights, the final set of SSA retrievals in the OMAERUV product are*

*reported at the mean ALH provided by the 30-month long averaged climatology developed using OMI-CALIOP combined observations (Torres et al., 2013). This mean climatological ALH is taken as the OMI algorithm ALH.*

RC: Figure 7. Very good and informative caption. They should all be this good.

*AC: We thank the reviewer for the comment.*

RC: Lines 372-373. This assumes that the OMI-MODIS retrieval is correction, which has not been proven. The wording is also awkward for me. What I would say is this: The most important observation from this analysis is that the operational OMI-only retrieval of SSA overestimates SSA when it also overestimates ALH, and vice-versa.

*AC: The sentence has been modified accordingly.*

RC: Lines 374-379. Does it matter whether or not the operational OMI uses CALIPSO climatology or the prior assumptions? Did you study this? I don't think so. The algorithm isn't using real-time collocated CALIPSO. It is using CALIPSO climatology. There could still be issues. Anyway, because you didn't actually study the difference between CALIPSO climatology and prior climatology, these details here are just distracting.

*AC: The details regarding the aerosol layer height assumption have been removed.*

RC: Lines 379-381. This sentence is very good and valuable.

*AC: We thank the reviewer for the comment.*

RC: Lines 382-390. I don't know understand the point the authors are trying to make here. The paragraph wanders.

*AC: The paragraph has been modified.*

RC: Line 396 is unfinished

*AC: The sentence has been modified.*

RC: Lines 391-404, and Figures 8 and 9. These are not earth-shattering results. We all know this. I don't have time to look back into the old Deep Blue papers, but this is the basis for that algorithm. \*\*\*\*\*I'm not opposed to including this analysis in the paper, but it has to be put into context with previous work. \*\*\*\* Also, I might combine Figures 8 and 9 into a single 2-panel figure.

*AC: The paragraph has been modified, and the figures have been combined. The modification is as follows “The basis of many aerosol retrievals by satellites in the UV spectrum is the sensitivity of aerosol absorption to Rayleigh scattering which acts as a bright background and contributes to the TOA radiance (Torres et al., 1998; 2002). Change in ALH can affect the TOA radiance since the aerosol layer will interact with the Rayleigh scattering due to molecules present in the atmosphere. However, this effect is smaller compared to the effect due to the change in AOD and SSA (Kim et al., 2018). Kim et al. (2018) also showed how the misclassification of aerosol type and size could affect ALH retrieval. OMI SSA retrievals which are based on LUT depend on the ALH assumed along with aerosol type. The SBDART simulations in the current work show how for a particular TOA flux, SSA varies with ALH when the other aerosol properties are kept constant.”*

RC: Figure 10 caption needs a lot more detail. What does each point represent in terms of spatial/temporal averaging? What is the correlation? Is there any correlation?

*AC: The caption has been changed with more explanation*

RC: Line 428. I think it is an accident that the MODIS-OMI mean matches the cruise exactly. The statistics tell the same story that I see with my eye: : : The two retrievals match the cruise about the same, to within their expected uncertainties.

*AC: After using the new version (1.8.9) of OMI, section 5.4 has been rewritten.*

RC: Section 5.4 as a whole. It’s dangerous to expect the total column ambient retrievals to match whatever was making in situ measurements at the ocean surface. Different everything. Some of these caveats need to be expressed in this section. \*\*\*\*Also and this is critical: : : we need to know what instrument was used on the cruise and exactly what it measured. What wavelength? What method? Did it dry aerosols or not? The name of the ship. Other things. Details here are essential.\*\*\*\*

*AC: We thank the reviewer for his suggestion. The following has been added*

*“During both the cruises, the aerosol sampling was done onboard the Oceanic Research Vessel Sagar Kanya. While the 2006 cruise covered both the Arabian Sea and the Bay of Bengal, the winter cruise of 2009 covered the Bay of Bengal. The cruise tracks are provided in detail in Moorthy et al., 2008 and 2010, respectively. The SSA values at different wavelengths were estimated from spectral values of the absorption coefficient and scattering coefficient, measured using the instruments Aethalometer (Magee Scientific AE-31, USA) and*



*an integrating nephelometer (TSI 3563, USA) respectively. More details about the instrument and measuring techniques including the uncertainties are provided in Nair et al. (2008). However, both the cruise did not estimate SSA values in the UV spectrum. The closest wavelength at which SSA was calculated is 450nm which has been used to compare with the satellite retrievals of SSA (388nm). Ground-based SSA estimates based on in-situ measurements are seldom consistent with columnar retrievals from satellites especially when elevated aerosols are present. This uncertainty along with the uncertainty in the assumption of SSA being uniform between 388nm and 450nm implies that the current comparison of study cannot be used as a validation study. Instead, it is used to understand the consistency of SSA retrievals from satellites with ground-based observations.”*

RC: Lines 457-458, or changes in ALH as the SAL cools and descends, right? I saw that gradient and I thought ALH right away, not changing aerosol properties.

*AC: The conclusion point has been modified as follows “The difference in SSA retrievals of both the algorithms ( $\Delta$ SSA) was found to be within  $\pm 0.03$  over ATL >80% of the time during all the seasons. Over the Arabian Sea, as seen in Satheesh et al. (2009),  $\Delta$ SSA was within the  $\pm 0.03$  range during MAM when the region was influenced by dust. The discrepancies during other season were due to the wrong assumption of aerosol layer height by OMI.”*

RC: Line 459. “OMI overestimates SSA at lower ALH and underestimates at higher values of ALH.” Sure, if the OMI-MODIS is true.

*AC: The statement has been modified as “seen that OMI overestimated SSA when it overestimated ALH and vice versa which can be attributed to the wrong assumption of aerosol height.”*

RC: Lines 459-463. \*\*\*\* Again, I don't think you can say anything about the differences between CALIPSO climatology versus prior climatology. This should not be here in the major conclusions. What I might say here is, “Despite the operational algorithm moving to CALIPSO climatology, we continue to find systematic differences in the algorithm's SSA-ALH retrieval, when compared with the more robust OMI-MODIS retrieval. This may be due to situations when CALIPSO climatology is missing and the algorithm reverts to prior assumptions, or more likely, it may be due to lingering uncertainties in ALH even when using the improved climatology.” \*\*\*\*

*AC: We thank for the reviewer for the suggestion. The point has been modified as follows “During winter, when the aerosols were present closer to the surface, OMI-MODIS was more consistent compared to OMI which may be due to scenarios where the CALIPSO climatology is absent and OMI uses its previous aerosol model assumptions. The difference could also be due to the uncertainties in ALH value even after the improvement in the OMI algorithm with the addition of CALIPSO climatology.”*

RC: Line 464-466. \*\*\*\*Again, we all already know this. It is strange to find it in the major conclusions. \*\*\*\*

*AC: The conclusion point has been removed.*

RC: Lines 467-470. \*\*\*\*I think you are writing the way you wished it turned out. What you actually found that there was no significant difference between the OMI and OMI-MODIS retrieval in matching the cruise data, although the overall mean OMI-MODIS SSA for the area and period showed virtually no bias against the cruise data, while the OMI-only retrieval mean was biased 0.013 too high. \*\*\*\*

*AC: The point has been modified as “While both the algorithms did not match the cruise estimate during most of the dust season due to the presence of elevated aerosols, in few cases during ICARB, OMI performed better than OMI-MODIS. OMI performed better due to the better assumption of dust model in the algorithm and (or) wrong model assumption by MODIS. During winter, when the aerosols were present closer to the surface, OMI-MODIS was a bit more consistent compared to OMI. This may be due to scenarios where the CALIPSO climatology is absent and OMI uses its previous aerosol model assumptions. This can also be due to uncertainties in ALH value even after the improvement in the OMI algorithm with the addition of CALIPSO climatology.”*

RC: Lines 471-472. I’m not sure about this point at all.

*AC: The corresponding point has been removed.*

RC: Line 474-475. \*\*\*\*What makes you say that the OMI-MODIS is able to detect absorbing aerosols much better than OMI? Detect is not the same as retrieving SSA. Keep that in mind. Note also in the global maps OMI has much better coverage than OMI-MODIS. Why? You never discussed that and it’s important. Is OMI reporting cloud contaminated results? Or is OMI much better at detection? \*\*\*\*

*AC: The following paragraph has been added “OMI retrieves aerosol properties at high cloud fraction (Gassó and Torres, 2016) implying two things, either OMI can detect aerosols present above clouds or the OMI pixel was prone to cloud contamination. In their study, Gassó and Torres (2016), observed that while MODIS cloud fraction can be used to screen out cloudy pixels in OMI, it cannot be the lone criterion. While they performed for a single case, an analysis of a larger spatial and temporal scale is required. Aerosol type and aerosol layer height play a vital role in the retrieval of aerosol properties. Without the assumption of aerosol type or height, OMI-MODIS can perform SSA retrievals which is consistent with cruise estimates during the winter when the Bay of Bengal is influenced by anthropogenic aerosols present close to the surface. This is not the case when dust aerosols are present. This discrepancy can be attributed to the difference in the aerosol model assumption by MODIS and OMI. This comparison study has very few points for a detailed analysis. Hence, an accurate comparison and validation of such retrieval algorithms can be possible only when there are more ground-based observations available in the UV spectrum on a larger spatial and temporal scale along with vertical profiles of aerosol absorption.*

## **Anonymous Referee #2**

### **Specific comments:**

RC: A similar study carried out by Gasso and Torres [2016] presents the results on deriving SSA and ALH from OMI-MODIS synergy and discusses the role of cloud contamination in OMI aerosol retrievals, which author misses to explain in greater details. A discussion highlighting important findings of Gasso and Torres [2016] and its (in)consistency with the new results presented in the paper is required.

*AC: We thank the reviewer for the comment. As suggested a discussion on the important findings of Gassó and Torres and its context in the current work has been included in the introduction and the results section.*

RC: Which version of the OMAERUV product does author use in the present study? I assume here that the latest OMAERUV version 1.8.9 has been employed here to derive the results. If not, the author needs to redo the entire analysis with the latest dataset which incorporates a number of changes applied to the previous version of the algorithm.

*AC: The version used initially was version 1.4.2. As suggested by the reviewer, the entire analysis has been redone using the latest OMAERUV version 1.8.9.*

### **Introduction:**

RC: A statement or two citing importance of SSA in estimating radiative forcing with appropriate reference would be needed in the introduction. Figure 5 can be used as a reference.

*AC: As suggested by the reviewer, the effect of change in SSA on the estimation of radiative forcing has been added in the introduction along with references. Figure 8 (Earlier Figure 5) has been used to show the importance of SSA through SBDART simulations.*

RC: Line 52-55: Author has completely forgotten to mention about the long-term record of aerosol absorption retrievals from AERONET!

*AC: Table 1 contains the different methods (along with the corresponding references) used by satellites and ground-based measurements to retrieve aerosol absorption (SSA) including AERONET.*

RC: Line 55: Remove “images”.

*AC: The word “images” has been removed*

RC: Line 63-65: It is assumed here that the author is referring to the AOD retrievals from satellites. In this case, the statement “they still have a limited success over deserts” is untrue; AOD retrievals over bright surfaces from the near-UV, Deep Blue, and MAIAC algorithms have achieved a great success in retrieving accurate AODs.

*AC: Here SSA retrievals are considered and based on Table 1, it can be seen that over bright surfaces, SSA retrievals have limited success.*

RC: Line 67-69: What do the “large surface reflectance contrasts” means?

*AC: The sentence has been modified as follows “SSA retrieval in UV spectrum hence avoids difficulties encountered over surfaces with high albedo.”*

RC: Line 72: The sub-pixel cloud contamination is a result of the larger footprint of size 13 x 24 kmsquare.

*AC: The reason for sub-pixel contamination has been mentioned in the introduction as suggested.*

RC: Line 76: The time difference between the observations from OMI and MODIS is about 7-8 minutes post-2008 period. A brief discussion about the OMI-MODIS combined retrieval approach is needed here.

*AC: As suggested by the reviewer a brief explanation of the OMI-MODIS algorithm has been mentioned in the introduction as follows “The algorithm uses the MODIS AOD as a reference to infer the aerosol layer height and SSA from OMI. This removes any a priori assumption made by the OMI algorithm regarding an aerosol model.”*

## **Section 2.1 First paragraph**

RC: In addition to the higher sensitivity to aerosol loading and its absorption properties, the 354 and 388 nm wavelengths have negligible interference from trace gases.

*AC: The statement has been modified as follows “The reason behind choosing these wavelengths is the high sensitivity of upwelling radiances to aerosol absorption and the lower influence of surface in measurements due to low reflectance values in the UV region. In addition to this, the wavelengths also have negligible interference from trace gases.”*

RC: “sulphate-based” aerosol type was a gross terminology used for the boundary layer aerosols; it should be changed to “background and urban-industrial” aerosol type.

*AC: The corrections have been made as suggested by the reviewer*

RC: Line 111: Rephrase the sentence as “the retrievals are performed reported for the five discrete aerosol layer heights, i.e., surface (exponential profile), 1.5, 3.0, 6.0, and 10.0 km with latter four following a Gaussian distribution. The final set of AOD/SSA/AAOD retrievals is reported at the mean ALH provided by the 30-month long averaged climatology developed using OMI-CALIOP combined observations.”

*AC: The sentence has been rephrased. Since the latest version of the product (v1.8.9) is used, a brief explanation regarding the changes in the new version has also been added.*

RC: Line 120: “have helped distinguish carbonaceous aerosols from dust particles”

*AC: The sentence has been rephrased.*

RC: Line 126: “An effective aerosol layer height was calculated using the CALIOP 1064 nm attenuated backscatter weighted by corresponding altitudes”

*AC: The sentence has been modified accordingly.*

RC: Line 128: “..in the OMAERUV retrievals which then validated against the AERONET observations”

*AC: The sentence has been rephrased.*

### **Section 3. Algorithm**

RC: MODIS aerosol product reports retrievals at 10 x 10 km spatial resolution at nadir.

*AC: The sentence has been modified.*

RC: Line 160: “..prone to sub-pixel cloud contamination which may result in overestimation in AOD and SSA”

*AC: The sentence has been modified accordingly.*

RC: Line 163: The high accuracy of size-resolved aerosol retrievals with MODIS is because the over-ocean algorithm employs all seven channels (0.47-2.13 micron) in the inversion enabling better characterization of fine and coarse particles.

*AC: The sentence has been rephrased as suggested by the reviewer.*

RC: Line 169: “..constraints the retrievals of AOD and SSA”

*AC: The sentence has been modified.*

RC: Line 179: Does the algorithm use Angstrom Exponent retrieved by MODIS over the ocean?

*AC: The algorithm does not use the Angstrom Exponent retrieved by MODIS. According to Satheesh et al. (2009), the equation used to correct the extrapolated MODIS AOD “corrects for the variable sensitivity of aerosol species to different ranges of the spectra” and is dependent on the amount of fine mode aerosols present. This equation was obtained by plotting the difference in MODIS and AERONET AOD with the difference in AOD at 470nm and 870nm (the difference represents the aerosol spectral curvature)*

## **Section 5. Results**

RC: Line 214-215: not a phenomenon, but the instrumental issue. While a brief discussion on row anomaly is provided in Jethva et al. [2014], Torres et al. [2018] discuss it in great details and its effect on the scan dependency on the OMAERUV retrievals.

*AC: The statement has been corrected. Explanation regarding the row anomaly issue along with the references is discussed in Section 2.1.*

### **Section 5.1**

RC: The differences could also be attributed to the shape of the dust particle. In the latest OMAERUV (V1.8.9) algorithm, dust is assumed to be of spheroidal shape with axis ratio distribution adopted from Dubovik et al [2006] study. Please refer to Torres et al. [2018] AMT paper; the citation is provided earlier in this report.

*AC: We thank the reviewer for the suggestion. As mentioned, the shape of the dust has also been added as a factor for the difference.*

## **Section 6. Summary and conclusion**

RC: In addition to the sub-pixel cloud contamination and ALH, an uncertainty in prescribing surface albedo is another source of error in the retrieval of SSA from space.

*AC: Uncertainty in surface albedo has been added in the list of issues involved in the retrieval of SSA.*

RC: 3. Is OMI unable to retrieve absorbing aerosols for low ALH or does retrievals but under/over-estimate SSA?

*AC: The statement has been corrected as follows “From Fig. 7 it is also seen that OMI overestimated SSA when it overestimated ALH and vice versa. This can be attributed to the wrong assumption of vertical profiles of aerosols.”*

RC: 5. Provide the statistics of the cruise vs. satellite comparison.

*AC: The statistics have been added.*

## **Figures**

RC: Figure 1. Since the dynamical range of SSA variations in these maps is confined to 0.85-1.0, a narrower color scale covering this range would be desirable.

*AC: A narrower colour scale from 0.85-1.0 has been used to represent global SSA maps.*

RC: Figure 2. For the most part, SSA retrieved from OMI-MODIS synergy is larger than that retrieved from OMI only.

*AC: After using the latest version of OMI, it was seen from Fig. 2 that the majority of OMI-MODIS retrievals was lesser than OMI especially during the JJA and SON seasons*

RC: Figure 4. From where does the author get ALH difference of 8-10 km?

*AC: There were some points over the two study regions, mostly in the open ocean and some near the coast, where the MODIS extrapolated AOD ( $AOD_{388}$ ) values were closer to the OMI algorithm values retrieved at 6km or 10km (based on linear interpolation). However, the final height given by OMI based on the climatology is lesser than  $\sim 3.5$ km. This resulted in the ALH difference to be  $> 6$ km. According to Gassó and Torres (2016), this could be due to the difference in MODIS AOD and OMI AOD spectral curvature resulting in unrealistic height estimation. However, this has not been explored in detail in the current work and will have to be looked in the future.*

RC: Figure 8. Add the measures of agreement, i.e., N, RMSD, correlation

*AC: The statistical measures of the agreement have been added. These include the Total number of points, RMSE and the correlation.*

RC: A plot demonstrating the effect of a change in AOD on the change in SSA either through radiative transfer calculations or from satellite data is needed here. The author may choose a



representative region here, say the tropical Atlantic Ocean with dust transport from Sahara for such analysis.

*AC: A plot between the change in AOD and change in SSA has been shown in Figure 6b. The following text has been added in the manuscript – “Gassó and Torres (2016), in their detailed analysis of the OMI UV aerosol product (version 1.4.2), studied the OMI-MODIS method for two specific cases. They have mentioned that when the extrapolated MODIS 388nm AOD was not within the OMI LUT values, the OMI-MODIS algorithm retrieves unrealistic height and SSA. For the ARBOB region, the difference in AOD ( $AOD_{MODIS} - AOD_{OMI}$ ) has been plotted with the difference in SSA ( $SSA_{OMI-MODIS} - SSA_{OMI}$ ) (Fig. 6b). The colorbar represents the difference in ALH ( $ALH_{OMI-MODIS} - ALH_{OMI}$ ) retrieved by both the algorithms. An inverse relation can be seen implying that when OMI underestimates AOD compared to MODIS, OMI overestimates SSA compared to OMI-MODIS. The difference in AOD is mainly within the  $\pm 0.5$  range. However, there are a few points where the AOD difference was  $> 3$ . Mostly in such cases, the difference between the ALH and SSA estimates of both the algorithms was high. However, there are points when the AOD difference was high, but the ALH and SSA differences were within  $\pm 1$  km and  $\pm 0.03$  respectively. Similarly, the difference between ALH and SSA values of both the algorithms was high when the AOD difference is within  $\pm 0.5$ . These discrepancies can be attributed to the AOD spectral curvature of an aerosol type assumed by MODIS which is different by the aerosol model assumed by OMI UV aerosol product (Gassó and Torres, 2016). Whether any other property apart from AOD and shape (for dust aerosols) can affect the ALH and SSA retrievals have to be studied in the future.”*

# 1 Multi-Satellite Retrieval of SSA using OMI-MODIS algorithm

2 Kruthika Eswaran<sup>1,2\*</sup>, Sreedharan Krishnakumari Satheesh<sup>1,2</sup> and Jayaraman Srinivasan<sup>1,2</sup>

3 <sup>1</sup> Centre for Atmospheric and Oceanic Sciences, Indian Institute of Science, Bangalore, India

4 <sup>2</sup> Divecha Centre for Climate Change, Indian Institute of Science, Bangalore, India

5 \*Correspondence to: Kruthika Eswaran (kruthika.eswaran89@gmail.com)

6 **Abstract** - Single scattering albedo (SSA) represents a unique identification of aerosol type and  
7 aerosol radiative forcing. However, SSA retrievals are highly uncertain due to cloud  
8 contamination and aerosol composition. The recent improvement in the SSA retrieval algorithm  
9 has combined the superior cloud~~-~~masking technique of the Moderate Resolution Imaging  
10 Spectroradiometer (MODIS) and the better sensitivity of the Ozone Monitoring Instrument  
11 (OMI) to aerosol absorption. The combined OMI-MODIS algorithm has been validated over a  
12 small spatial and temporal scale only. The present study validates the algorithm over global  
13 oceans for the period 2008-2012. The geographical heterogeneity in the aerosol type and  
14 concentration over the Atlantic Ocean, the Arabian Sea and the Bay of Bengal was useful to  
15 delineate the effect of aerosol type on the retrieval algorithm. We also noted that OMI  
16 overestimated SSA when absorbing aerosols were present closer to the surface. We attribute this  
17 overestimation to data discontinuity in the aerosol height climatology derived from Cloud-  
18 Aerosol Lidar and Infrared Pathfinder Satellite Observations (CALIPSO) satellite. OMI uses pre-  
19 defined aerosol heights over regions where CALIPSO climatology is not present leading to  
20 overestimation of SSA. The importance of aerosol height was also studied using the Santa  
21 Barbara DISORT radiative transfer (SBDART) model. The results from the joint retrieval were  
22 validated with ground-based measurements and it was seen that OMI-MODIS SSA retrievals  
23 performed better than OMI only retrieval [over the Bay of Bengal during winter when the](#)

24 [aerosols are present closer to the surface. Discrepancy between satellite retrievals and cruise](#)  
25 [measurements was seen when elevated aerosols are present which might not be detected by the](#)  
26 [cruise instruments.](#)

## 27 **1. Introduction**

28 Aerosols of different types are spatially distributed heterogeneously and at different altitudes in  
29 the atmosphere. Depending upon their properties, certain aerosols (biomass and carbon) warm  
30 the atmosphere by absorbing radiation, while other aerosols (sea salts and sulphates) cool the  
31 atmosphere by scattering radiation (Ramanathan et al., 2001). Due to the opposing effects on the  
32 atmosphere aerosols can have either net warming or cooling effect on the global climate  
33 depending upon the aerosol type, concentration and vertical distribution. Effect of [natural and](#)  
34 [anthropogenic](#) aerosols on the global climate is measured by 'aerosol radiative forcing' (the  
35 perturbation to the earth's radiation budget caused by the presence of aerosols). Positive forcing  
36 implies atmospheric warming and vice-versa. (Liao and Seinfeld, 1998; Podgorny and  
37 Ramanathan, 2001; Satheesh, 2002; Johnson et al., 2003; Kim et al., 2004; Moorthy et al., 2004;  
38 Meloni et al., 2005; Satheesh and Moorthy, 2005; Seinfeld and Pandis, 2006; Satheesh et al.,  
39 2008; Chand et al., 2009; Mishra et al., 2015). According to the climate assessment report, the  
40 estimation of aerosol radiative forcing ([due to anthropogenic aerosols](#)) is a major cause of  
41 uncertainty in the estimation of climate sensitivity and therefore presents a ~~great~~-[significant](#)  
42 impediment to climate modelling (IPCC, 2013). The uncertainty is ~~largely~~-[mostly](#) due to the lack  
43 of accurate measurement of the scattering and absorbing properties of the aerosols (Cooke and  
44 Wilson, 1996; Menon et al., 2002; Chung and Seinfeld, 2002; Bond and Sun, 2005).

45 The Single Scattering Albedo (SSA), (the fraction of [the total extinction of radiation](#)  
46 [attributed to scattering](#)~~radiation scattered out of total extinction of radiation~~) is used to

47 distinguish the scattering and absorbing properties of aerosols. SSA represents a unique  
48 fingerprint of the type of aerosol and its radiative forcing (Hansen et al., 1997; Haywood et al.,  
49 1997; Myhre et al., 1998). In general, purely scattering aerosols have SSA value of  
50 approximately 1 while highly absorbing aerosols have SSA less than 0.7. However, [SSA](#)  
51 [retrievals](#)~~SSA values~~ lack high certainty (Bond and Bergstrom, 2006; Bond et al., 2013).  
52 Uncertainties in SSA ~~measurements~~[retrievals](#) are due to factors such as cloud contamination,  
53 instrumentation error and aerosol modification due to atmospheric processes. [A small change in](#)  
54 [SSA can cause the aerosol radiative forcing to change from negative to positive \(Hansen et al.,](#)  
55 [1997; Seinfeld and Pandis, 2006\). Loeb and Su \(2010\) performed a radiative perturbation](#)  
56 [analysis and found that direct aerosol radiative forcing was highly sensitive to small](#)  
57 [perturbations in SSA under clear-sky and cloudy-sky conditions. A simulation study using Santa](#)  
58 [Barbara DISORT Radiative Transfer \(SBDART\) model in the present work \(Section 5.3\) shows](#)  
59 [that a change in SSA from 0.8 to 1 can induce a change of 4 Wm<sup>-2</sup> in the top-of-atmosphere](#)  
60 [\(TOA\) flux depending on the aerosol type and aerosol layer height \(Figure 8\).](#) Better SSA  
61 retrievals (both in-situ and satellite-based) are required to reduce the uncertainty in SSA for a  
62 more accurate estimation of aerosol forcing; particularly over regions influenced by a variety of  
63 air masses. There is also a need for accurate spectral aerosol absorption measurements, which is  
64 required to validate SSA derived from satellite~~measurements~~[s](#) (Bergstrom et al., 2007).

65 Studies on the various ~~direct~~ measurements of ~~SSA~~[aerosol light absorption using instruments](#)  
66 and their uncertainty evaluation have been performed previously (Horvath, 1993, Heintzenberg  
67 et al., 1997; Moosmuller et al., 2009). [The different methods of retrieval of SSA, both ground-](#)  
68 [based and using satellites, are provided in Table 1. Unlike aerosol absorption coefficient, SSA is](#)  
69 [not measured directly by an instrument. Instead, it is retrieved using lookup tables or estimated](#)

70 using other parameters which are measured or calculated using models. ~~Along with ground-~~  
71 ~~based retrievals of SSA, there have been other indirect methods to retrieve the parameter using~~  
72 ~~satellite images and observations (Table 1).~~

73 Though these previous studies on ground-based ~~measurements~~ retrievals have brought a  
74 fundamental understanding to the estimation of amounts of aerosols / aerosol chemistry, their  
75 restricted spatial and temporal extent is a ~~major~~ significant limitation. Moreover, these studies  
76 have reduced availability of scenes for indirect retrievals. Some techniques are limited due to  
77 cloud contamination while others operate only under specific conditions (e.g. presence of sun  
78 glint). This presents a need for better SSA retrieval algorithms that overcome the present  
79 technical limitations and that can be applied on a global scale. The global extent of observations  
80 from satellites has increased the spatial extent of the observations (Kaufman et al., 2002a).  
81 Though the satellite-based SSA retrievals have been shown to be extremely successful over the  
82 majority of ocean and land regions, they still have a limited success over deserts and ice sheets.  
83 Over deserts and ice-sheets, high surface reflectance affects the satellite retrievals in the visible  
84 spectrum. To counter this, SSA is retrieved in the UV spectrum (330 nm to 400 nm) over these  
85 regions (Torres et al., 1998, 2007). In the UV spectrum, the upwelling radiances are highly  
86 sensitive to the aerosol absorption and also have a lower influence of surface albedo (Torres et  
87 al., 2007). SSA retrieval in UV spectrum ~~also~~ hence avoids difficulties encountered ~~in scenarios~~  
88 ~~where there are large surface reflectance contrasts~~ over surfaces with high albedo.

89 The quality of OMI SSA retrievals is affected by sub-pixel cloud contamination (due to the  
90 larger footprint of size 13km x 24km) and the spectral surface albedo (Torres et al., 2007). To  
91 counter the problems and uncertainties in the OMI SSA retrieval (Table 2), Satheesh et al. 2009  
92 used retrievals from multiple satellites. They used combined retrievals from OMI-MODIS since

93 ~~sensors on each of the satellites~~ each of these sensors have their own strengths and both fly within  
94 ~~~7-8~~ ~~few~~ minutes of each other in the A-train constellation (Stephens et al., 2002). The better  
95 cloud-screened retrieval of AOD from MODIS (Levy et al., 2003) and the high sensitivity of  
96 OMI to aerosol absorption was used to develop a hybrid algorithm to retrieve SSA (Satheesh et  
97 al., 2009). The algorithm uses the MODIS AOD as a reference to infer the aerosol layer height  
98 and SSA from OMI. This removes any a priori assumption made by the OMI algorithm  
99 regarding an aerosol model. The study by Satheesh et al. 2009 was performed over the East  
100 tropical Atlantic Ocean, the Central tropical Atlantic Ocean and the Arabian Sea for the year  
101 2006. A comparison of the retrieved aerosol height with aircraft measurements showed that OMI-  
102 MODIS was more accurate than OMI. Gassóe and Torres (2016) performed a detailed analysis of  
103 the OMI UV product retrievals over oceans and island sites. They compared the OMI retrieved  
104 AOD with MODIS and AERONET (Aerosol Robotic Network) AODs. ~~This work~~ They also used  
105 the OMI-MODIS algorithm for only two particular cases over and near Africa to understand how  
106 the assumption of aerosol height and shape affected AOD and SSA retrievals. It was found that  
107 when the actual height from satellite Lidar was used instead of climatological values and when  
108 the shape of dust aerosols was assumed to be non-spherical, the retrievals by OMI agreed better  
109 with other observations including the original OMI-MODIS method. ~~While the~~ The OMI-MODIS  
110 algorithm has been used in calculating aerosol radiative forcing (Satheesh et al., 2010) over  
111 oceanic regions surrounding India and used in retrieving SSA over land (Narasimhan and  
112 Satheesh, 2013) as well as used to understand the retrievals of OMI UV products for two  
113 particular cases (Gassóe and Torres, 2016). ~~),~~ However, a detailed analysis of the algorithm on a  
114 larger spatial and temporal scale has not been done so far.

115 The current work applies the OMI-MODIS algorithm to retrieve SSA on a global scale. It is

116 applied over [the](#) global oceans from 2008-2012. Regional analysis over the Atlantic, the Arabian  
117 Sea and the Bay of Bengal ~~has been~~are done by incorporating the aerosol layer height and the  
118 type of aerosols. ~~A simulation study using Santa Barbara DISORT Radiative Transfer (SBDART)~~  
119 ~~model was performed to highlight the importance of aerosol layer height.~~ After estimating SSA  
120 values using the OMI-MODIS algorithm, the present study then uses cruise measurements of  
121 SSA from the Integrated Campaign for Aerosols, Gases and Radiation Budget (ICARB) and  
122 winter ICARB campaigns over Arabian Sea and Bay of Bengal in 2006 and 2009 to validate the  
123 same (Moorthy et al., 2008, 2010).

## 124 **2. Data**

### 125 **2.1. OMI**

126 The Ozone Monitoring Instrument (OMI) onboard the Aura satellite was launched in 2004. For  
127 OMI measurements two aerosol inversion schemes are used- OMI near UV (OMAERUV)  
128 algorithm and the multi-wavelength (OMAERO) algorithm (Torres et al., 2007). The OMAERO  
129 algorithm uses 19 wavelengths in the range of 330-500 nm to retrieve corresponding aerosol  
130 characteristics. For the present study, we have used the OMAERUV algorithm which uses  
131 measurements at two wavelengths 354 nm and 388 nm. The reason behind choosing these  
132 wavelengths is the high sensitivity of upwelling radiances to aerosol absorption and the lower  
133 influence of surface in measurements due to low reflectance values in the UV region. [In addition](#)  
134 [to this, the wavelengths also have negligible interference from trace gases.](#) This gives a unique  
135 advantage of retrieving aerosol properties over ocean and land including arid and semi-arid  
136 regions (Torres et al., 1998; 2007).

137 The products derived from the algorithm include AOD, absorption aerosol optical depth  
138 (AAOD) and single scattering albedo (SSA). These are derived from pre-computed reflectance

139 values for different aerosol models. Three major types of aerosols have been used - Desert dust,  
140 carbonaceous aerosols from biomass burning and ~~sulphate-based~~[background and urban-industrial](#)  
141 aerosols. Each type has seven models of SSA. The retrieved products of OMAERUV are  
142 sensitive to the aerosol layer height (Torres et al., 1998)- ~~and are reported for five discrete~~  
143 ~~aerosol layer heights, i.e., surface (exponential profile), 1.5, 3.0, 6.0, and 10.0 km with latter four~~  
144 ~~following a Gaussian distribution. The values are derived at surface and at 1.5, 3.0, 6.0 and 10.0~~  
145 ~~km above the surface. The best estimate of the values of AOD, AAOD and SSA of a particular~~  
146 ~~choice of aerosol vertical distribution are evaluated.~~

147 Due to the high sensitivity of SSA retrieval to the assumption of aerosol height and aerosol  
148 type ([Torres et al., 2002](#)), the OMI algorithm was improved (Collection 003-PGE V1.4.2, Torres  
149 et al., 2013). ~~The~~[using](#) climatology of aerosol layer height from CALIPSO (Cloud-Aerosol Lidar  
150 and Infrared Pathfinder Satellite Observations) along with carbon monoxide (CO) measurements  
151 from AIRS (Atmospheric Infrared Sounder) [have helped distinguish carbonaceous aerosols from](#)  
152 ~~dust particles for better identification of carbonaceous aerosols~~. Torres et al. (2013) showed that  
153 the combined use of AIRS CO measurements and OMI Aerosol Index (AI) retrievals, helped in  
154 identifying the type of absorbing aerosol. Thus, smoke layers were identified when values of AI  
155 and CO measurements were high and during events of high AI and low CO values, the aerosols  
156 were identified as dust. The AIRS CO measurements were also used to identify large aerosol  
157 loading which was otherwise represented as clouds by the OMAERUV algorithm. Using  
158 collocated observations of OMI and [Cloud-Aerosol Lidar with Orthogonal Polarization](#)  
159 [\(CALIOP\)](#), Torres et al. (2013) estimated the height of elevated absorbing aerosols for a 30-  
160 month period from July 2006 to December 2008. [An effective aerosol layer height was](#)  
161 [calculated using the CALIOP 1064 nm attenuated backscatter weighted by corresponding](#)



162 ~~altitudes~~An effective aerosol height was calculated from the attenuated backscatter weighted  
163 ~~with average height using the CALIOP 1064 nm measurements.~~ The 30-month climatology of  
164 aerosol height was used in the OMAERUV retrievals which then validated against the  
165 AERONET observations~~algorithm and validated with Aerosol Robotics Network (AERONET)~~  
166 ~~observations~~ (Torres et al., 2013). The results showed that there was an improvement in the  
167 retrievals. ~~The original aerosol height assumptions were used in the algorithm over regions~~  
168 ~~where the climatology was unavailable.~~

169 Since 2007, observations have been affected by an instrumental issue called the row  
170 anomaly which reduces the quality of radiance at all wavelengths (Jethva et al., 2014). Torres et  
171 al. (2018) studied the impact of row anomaly on the OMAERUV retrievals by comparing  
172 monthly values AOD, SSA and UV aerosol index (UVAI) of two different sets of scattering  
173 angles. Over regions dominated by carbonaceous and sulphate aerosols, the agreement between  
174 the sets was better than over arid regions dominated by dust aerosols. Differences were also  
175 found over cloudy regions. The discrepancies were attributed to the inaccurate representation of  
176 scattering effects of dust aerosols and cloud droplets. Better representation of scattering by  
177 clouds and the non-spherical (spheroidal) shape assumption of dust aerosols was found to reduce  
178 the inconsistencies in aerosol products due to row anomaly. These improvements have been  
179 incorporated in the latest version of OMAERUV product (version 1.8.9) which has been used in  
180 the present study. Along with the aerosol products retrieved at different heights, the final set of  
181 AOD/SSA/AAOD retrievals in the OMAERUV product is reported at the mean ALH provided  
182 by the 30-month long averaged climatology developed using OMI-CALIOP combined  
183 observations (Torres et al., 2013). The original aerosol height assumptions were used in the  
184 algorithm over regions where the climatology was unavailable.~~For the present study we have~~

185 ~~used the improved OMAERUV algorithm along with AOD, SSA retrievals at different aerosol~~  
186 ~~heights and as well as the best estimates of AOD and SSA.~~

## 187 **2.2. MODIS**

188 The Moderate Resolution Imaging Spectrometer (MODIS) instrument ~~in~~ on the Aqua  
189 satellite was launched in 2002. This instrument, with 36 spectral channels has a unique ability to  
190 retrieve aerosol properties with better accuracy over both land and ocean (Remer et al., 2005;  
191 Levy et al., 2003). Of these, seven channels (0.47-2.13  $\mu\text{m}$ ) are used to retrieve aerosol  
192 properties over the ocean (Tanré et al., 1997).

193 As described in Remer et al., (2005), before the retrieval algorithm, masking of sediments,  
194 clouds and ocean glint is performed to separate valid pixels from bad ones. The retrieval  
195 algorithm of MODIS (also called the inversion procedure) has been described in detail  
196 previously (Tanré et al., 1997; Levy et al., 2003; Remer et al., 2005). The algorithm uses a  
197 'look-up table' (LUT) approach, i.e., for a set of aerosol and surface parameters, radiative  
198 transfer calculations are performed. Spectral reflectance derived from the LUT is compared with  
199 MODIS-measured spectral reflectance to find the 'best' (least-squares) fit. The resulting  
200 combination of modes provides the aerosol model from which size distribution, properties  
201 including spectral optical depth, effective radius etc. ~~is~~ are derived. The product used from  
202 MODIS is the Level 2 aerosol (MYD04, Collection 5.1) product. The parameter chosen is  
203 'Effective\_Optical\_Depth\_Average\_Ocean' which provides the aerosol optical depth over the  
204 ocean at seven wavelengths. The value is the average of all the solutions in the inversion  
205 procedure with the least-square error  $< 3\%$ .

206 A combination of OMI and MODIS helps indirectly in counteracting the cloud  
207 contamination problem and also uses the strength of the individual sensors – OMI's sensitivity to

208 aerosol absorption combined with the better cloud screening of MODIS and accurate retrieval of  
209 AOD, and aerosol size (Satheesh et al., 2009; Narasimhan and Satheesh, 2013).

### 210 3. Algorithm

211 MODIS aerosol product reports retrievals at 10 x 10 km spatial resolution at nadir~~MODIS has~~  
212 ~~high spatial pixel resolution of 10km x 10km at nadir~~ (and a cloud mask at 500m and 1km  
213 resolution) whereas OMI ~~has a resolution of reports at~~ 13 km x 24 km. This results in ~~a~~ an OMI  
214 pixel being prone to cloud contamination which may result in an overestimation in AOD and  
215 SSA ~~which overestimates AOD and underestimates single scattering co-albedo (1-SSA)~~ (Torres  
216 et al., 1998). However, AAOD can be retrieved in the presence of small cloud contamination  
217 since there is cancellation of errors (Torres et al., 2007).

218 The high accuracy of size-resolved aerosol retrievals with MODIS is because the over-ocean  
219 algorithm employs all seven channels (0.47-2.13 micron) in the inversion enabling better  
220 characterization of fine and coarse particles.~~The higher accuracy in MODIS retrieval over ocean~~  
221 ~~is due to the fact that it has large number of channels in the Shortwave Infrared (SWIR) region~~  
222 ~~(TanreTanré et al., 1997; Remer et al., 2005; Levy et al., 2003).~~ While OMI is highly sensitive to  
223 aerosol absorption in the near-UV region, the accuracy in the retrieval of AAOD depends on the  
224 aerosol layer height assumption. OMI provides AOD and AAOD at different heights as  
225 prescribed by various aerosol types (Torres et al., 2007).

226 The assumption of aerosol layer height in the OMI algorithm ~~restricts~~ constraints the  
227 retrievals of AOD and ~~AAOD~~ SSA. ~~Using this as basis, the~~ The approach proposed in Satheesh et  
228 al. (2009) used MODIS AOD as an input to the OMI retrieval algorithm, so that the MODIS  
229 AOD constraints the OMI inversion so that the OMI inversion is free~~inversion, now checked, can~~  
230 ~~use the information~~ to infer the aerosol layer height and SSA. ~~To know the SSA at 388 nm, the~~

231 ~~AOD used should also be at the same wavelength.~~ Satheesh et al. (2009) extrapolated MODIS  
232 AOD [from the visible to 388nm](#) and compared the estimated UV AOD with high quality ground-  
233 based AERONET observations. The deviation between ~~MODIS~~[linearly](#)-extrapolated [MODIS](#)  
234 AOD and AERONET AOD was ~~greater~~[more significant](#) at higher AERONET AOD values. This  
235 was attributed to the presence of [a large number of fine-mode aerosols which caused a nonlinear](#)  
236 [curvature to the AOD spectral dependence and](#) affected AOD at UV wavelengths. Hence to  
237 improve the linear extrapolation, information on the aerosol spectral curvature was also included.  
238 This was achieved by using an average regression equation to correct the MODIS AOD  
239 (Satheesh et al., 2009; Equation 3). They showed that MODIS AOD [could be first](#) linearly  
240 extrapolated to 388 nm and ~~use the~~[then](#) corrected [for curvature before being used](#). ~~AOD~~ as input  
241 to the OMI retrieval algorithm. The present work uses the same algorithm as proposed by  
242 Satheesh et al. (2009) to retrieve SSA over the oceans for the region 60S-60N and 180W-180E  
243 from December 2007-November 2012. The methodology is described in detail in the following  
244 section.

#### 245 4. Methodology

246 The AOD for ocean obtained from the Level 2 aerosol product of [Aqua-MODIS \(MYD04\)](#) was  
247 used. Using linear extrapolation [with spectral curvature correction \(Satheesh et al., 2009\)](#), AOD  
248 at 388 nm (hereafter, AOD<sub>388</sub>) was calculated from AOD at seven wavelengths ranging from  
249 0.47-2.13  $\mu\text{m}$ , ~~after the inclusion of aerosol spectral curvature defined in Satheesh et al. (2009).~~  
250 OMI provides AOD and SSA for five different aerosol layer heights starting from [the](#) surface and  
251 at 1.5, 3.0, 6.0 and 10.0km (AOD<sub>OMI</sub> and SSA<sub>388</sub>). It also provides the best estimate of SSA  
252 calculated ~~for a particular aerosol vertical distribution~~[based on the CALIOP aerosol layer height](#)  
253 [climatology](#) (SSA<sub>OMI</sub>).

254 For the present study, polar regions are not included and hence pixels from both OMI and  
255 MODIS that are outside the 60S-60N and 180W-180E region are excluded. Pixels with invalid or  
256 missing values are also excluded. ~~To reduce computation time~~ The various parameters extracted  
257 from the data were re-gridded onto a uniform grid of  $0.5^\circ \times 0.5^\circ$  within the region of study to  
258 reduce computation time. For both the satellites, this procedure was repeated for each swath data  
259 which were then combined to calculate the daily means.

260 The daily data from collocated MODIS and OMI were utilised in the final algorithm. As  
261 mentioned before OMI provides AOD and SSA for five different aerosol layer heights. Using  
262 AOD<sub>388</sub> as the reference, the corresponding aerosol layer height was calculated from the five  
263 AOD<sub>OMI</sub> values through linear interpolation. This height is then used as a reference to find the  
264 SSA using interpolation from the set of SSA<sub>388</sub> values. Finally, this SSA (SSA<sub>OMI-MODIS</sub>), and the  
265 best estimate of SSA (SSA<sub>OMI</sub>) were compared ~~to~~ with each other.

## 266 5. Results

267 The spatial distribution of SSA retrieved using OMI is shown in Fig. 1a. The values are averaged  
268 over five years and plotted seasonally.

269 The SSA retrieved using OMI-MODIS algorithm is shown in Fig. 1b.

270 SSA over open oceans is close to 1 due to the presence of a large amount of sea-salt and  
271 sulphate. Closer to land, a variety of aerosols are present which results in SSA varying from  
272 ~~0.75~~ 0.85 to  $\sim 1$ . Over the oceans, ~~separating~~ separation of ocean colour effects and aerosol  
273 concentrations is difficult. Hence the OMI algorithm retrieves ~~only if there are~~ when enough  
274 absorbing aerosols are present, i.e. AI  $\geq 0.8$  (Torres et al., 2013). Only pixels whose quality has  
275 been assigned as 0 or the highest quality by OMI have been used. ~~Since 2007, observations have~~  
276 ~~been affected by a phenomenon called the row anomaly which reduces the quality of radiance at~~

277 ~~all wavelengths.~~ The points flagged for row anomaly are [also](#) not used in this study. ~~Further~~  
278 ~~information about row anomaly can be found in Jethva et al. (2014).~~ Thus, the retrievals did not  
279 cover the entire globe. From Fig.1a it can be seen that majority of the valid SSA retrievals were  
280 over major aerosol sources in the world and not over remote oceanic regions like central  
281 equatorial Pacific or Antarctic ocean. The major sources include the vast biomass outflow over  
282 the Atlantic Ocean from the west coast of Africa, the dust over the Arabian Sea from the arid  
283 areas of Arabia & Africa and the dust blown over the Atlantic Ocean from [the](#) Sahara. Other  
284 regions like the east coast of China, the Bay of Bengal are influenced by a variety of  
285 anthropogenic aerosols during different seasons. [In the OMI-MODIS algorithm, the aerosol layer](#)  
286 [height is retrieved through linear interpolation of AOD<sub>OMI</sub> at five different heights and AOD<sub>388</sub> as](#)  
287 [a reference. Linear interpolation was not performed for OMI retrievals which had a missing](#)  
288 [value at any particular height or if the OMI retrieval was the same at all heights. Such OMI-](#)  
289 [MODIS values were considered to be invalid. Similarly, if the MODIS AOD was found to be](#)  
290 [missing or invalid, the corresponding OMI-MODIS retrieval was also considered invalid. This](#)  
291 [resulted in a reduction in the total number of valid points in OMI-MODIS algorithm when](#)  
292 [compared to OMI algorithm \(Fig. 1b\). However, ~~B~~both the algorithms capture the major oceanic](#)  
293 regions which are influenced by [a](#) large number of aerosols. [Gassó and Torres \(2016\) for a](#)  
294 [particular day over the North Central Atlantic compared the AOD values retrieved by OMI and](#)  
295 [MODIS. They compared the difference with the aerosol cloud mask retrieved by MODIS. It was](#)  
296 [found that while most of the retrievals of OMI screened the cloudy pixels, some of the best](#)  
297 [quality \(flag=0\) pixels were found to be cloud contaminated. This they attributed to the coarser](#)  
298 [pixel size of OMI compared to the smaller pixel size of MODIS cloud product. At higher cloud](#)  
299 [fraction, OMI retrieved values implying that they can detect aerosol above clouds or the pixels](#)

300 [are prone to cloud contamination. Gassó and Torres concluded that only MODIS cloud fraction](#)  
301 [could not be used to screen out OMI pixels. A larger spatiotemporal scale of such an analysis is](#)  
302 [required but is beyond the scope of this manuscript and will be addressed in the future. However,](#)  
303 [OMI retrievals at higher cloud fraction could be the reason for more points in Fig. 1a than OMI](#)  
304 [MODIS in Fig. 1b.](#)

305 Two important regions over oceans influenced by a variety of aerosols are the [tropical](#)  
306 Atlantic Ocean and the oceans around the Indian subcontinent. The new approach was used over  
307 these regions- Atlantic (5N-30N; 60W-20W) (ATL) and Arabian Sea and Bay of Bengal (0-25N;  
308 55E-100E) (ARBOB).

### 309 **5.1. Difference in SSA retrieval algorithms during different seasons**

310 To understand how the OMI-MODIS algorithm ~~compared~~[compares](#) with the retrieval using [the](#)  
311 existing OMI algorithm, the difference between  $SSA_{\text{OMI-MODIS}}$  and  $SSA_{\text{OMI}}$  ( $\Delta SSA$ ) averaged  
312 over five years for different seasons is shown in Fig. 2.

313 During March-April May (MAM) and June-July-August (JJA), there is a longitudinal  
314 gradient in  $\Delta SSA$  from the coast of Sahara towards the open Atlantic Ocean. Kaufman et al.  
315 (2002a) showed that close to the coast of Africa, aerosols are more absorbing than those away  
316 from the coast. The difference in the type of aerosols as we move away from the coast could be  
317 one of the reasons for the gradient in  $\Delta SSA$ . [The difference can also be attributed to the shape of](#)  
318 [dust aerosols which are present in large numbers near the coast of Africa \(Torres et al., 2018\).](#)  
319 The  $\Delta SSA$  changes sign with season. This was attributed ~~to the dominating presence of either~~  
320 ~~natural aerosols (JJA) or anthropogenic aerosols (DJF)~~[to the change in aerosol layer height and](#)  
321 [\(or\) aerosol physical and optical properties.](#)

322 Both ATL and ARBOB regions are influenced by the type of aerosols which result in a

323 complex mixture and eventually resulting in the variation in SSA distribution over each season.  
324 While the spatial plot of  $\Delta$ SSA in Fig. 2 represents the regions where maximum and minimum  
325 differences are located around the globe, a distribution plot provides the ranges of  $\Delta$ SSA which  
326 dominate and which do not. The distribution of  $\Delta$ SSA for different seasons averaged over five  
327 years (2008-2012) is plotted in Fig. 3a and 3b for the regions- ATL and ARBOB respectively.

328 ~~DJF shows a strong positive bias in both the regions, JJA shows a negative bias and the~~  
329 ~~other two seasons show negligible bias. While dust outflows dominate over ATL, over ARBOB—~~  
330 ~~Arabian Sea is affected by dust at higher altitudes and sea salt near the surface whereas the Bay~~  
331 ~~of Bengal is influenced mainly by continental and marine aerosols. Over the tropical Atlantic~~  
332 Ocean,  $\Delta$ SSA was found within  $\pm 0.03$  >80% of the time during all the seasons. Over Arabian Sea  
333 and Bay of Bengal, the values of SSA matched within  $\pm 0.03$  during MAM when dust is present  
334 in large quantity over the region. However,  $\Delta$ SSA has values lower than  $< -0.03$  especially during  
335 the seasons of JJA and SON. Satheesh et al. (2009) showed in their analysis that the reason for  
336 the discrepancies during non-dust seasons could ~~The change in the sign of difference could either~~  
337 ~~be due to the difference in type of aerosol or the~~ be due to the wrong assumption ~~in~~ of aerosol  
338 layer height (ALH) or due to the wrong assumption of aerosol model. ~~To understand what type~~  
339 ~~of aerosols affect these water bodies,~~ Before understanding the role of ALH in SSA retrieval, the  
340 meteorological conditions of the ARBOB region (Arabian Sea and Bay of Bengal separately), for  
341 different seasons are studied and trajectory analysis is done. This helps in identifying major  
342 sources of aerosols during each season.

## 343 5.2. Trajectory analysis

### 344 5.2.1. ~~Atlantic (ATL)~~

345 ~~The region in the tropical Atlantic is surrounded by the Sahara Desert in the east and the~~



346 North America in the west. The transport of dust from Sahara over Atlantic Ocean is a regular  
347 occurrence (Prospero and Carlson, 1972). Aerosol distribution over Atlantic is also affected by  
348 the African Easterly Waves and other atmospheric dynamics in Africa (Zuluaga, 2012). The  
349 Atlantic region is influenced by not only dust from Sahara, but also by aerosols from biomass  
350 burning off the coast of Africa and aerosols from industries and pollution from America. Thus,  
351 there is a complex mixture of aerosols over the Atlantic Ocean during any season. A 7-day back  
352 trajectory analysis was performed at a location in the box (15N; 45W) using the online Hybrid  
353 Single Particle Lagrangian Integrated Trajectory (HYSPLIT) model for the years 2009-2010.  
354 The trajectory was computed for different seasons at 3 heights—500m, 1500m and 2500m above  
355 mean sea level (MSL). The Atlantic Ocean was divided into four quadrants representing the  
356 regions of possible sources of aerosols 1) North America, 2) Central/South America, 3) North  
357 Africa and 4) Southern Africa (Fig. 4). The influence of these aerosol sources over Atlantic  
358 Ocean is estimated as the percentage of trajectories that start from each region respectively. The  
359 maximum influence is given in bold (Table 2).

360 From Table 2 it can be seen that the major source of aerosols over the Atlantic Ocean is the  
361 dust outflow from the Sahara Desert (Prospero, 1996). Extreme heating over Sahara creates a  
362 layer of instability (Saharan Air Layer) which lifts the dust particles enabling long range  
363 transport. Far off the coast the warm dust layer encounters a cooler, wetter air layer causing  
364 inversion. This results in the dust layer being intact over Atlantic Ocean (Prospero and Carlson,  
365 1972). Field experiments like the trans Atlantic Aerosol and Ocean Science Expeditions  
366 (AEROSE I and II) showed the outflow of dust during spring and summer along with other trace  
367 gases and biomass aerosols (Morris et al., 2006). However, dust is not the only aerosol present in  
368 the region of study. Using an airborne differential absorption LIDAR (DIAL) system, Harriss et

369 al. (1984), found that there is advection of anthropogenic pollutants from North America to the  
370 North Atlantic Ocean. Advanced very high resolution radiometer (AVHRR) instrument on the  
371 National Oceanic and Atmospheric Administration (NOAA) 11 satellite provides global aerosol  
372 information. From that data it was found that large plumes over Atlantic Ocean were attributed to  
373 the pollution from North America and Europe. During spring and summer, the large outflow was  
374 due to the dust outbreak from Sahara and Sahel. Biomass burning from southern Africa, South  
375 America and anthropogenic emissions from North and Central America dominated the aerosol  
376 loading over Atlantic Ocean during winter (Husar et al., 1997). The MODIS instrument onboard  
377 the Terra satellite was first used to study the transport and deposition over Atlantic Ocean. It was  
378 found that during winter, the dust which was present was mixed with the biomass aerosols from  
379 Sahel and closer to the coast of North America the dust was influenced by the pollution and  
380 smoke from the continent. Pure dust was present over the ocean during summer months  
381 (Kaufman et al., 2005). From Table 2 it is also seen that the dust dominated at all heights except  
382 during winter when the pollution from North America dominated at higher altitudes.

### 383 **Arabian Sea and Bay of Bengal (ARBOB)**

384 The Arabian Sea and the Bay of Bengal are oceanic regions on the west and east coast of  
385 India respectively. Both regions are influenced by various types of aerosols during different  
386 seasons. The Arabian Sea has been dominated by dust aerosols and is influenced by high levels  
387 of dust during certain seasons as seen from satellite images (Sirocko and Sarnthein, 1989). Pease  
388 et al. (1998) studied the geochemistry and the transport of various dust samples during different  
389 cruises in different seasons. During winter and summer, the pattern of aerosol transport was  
390 similar to that of the Indian monsoon pattern – northeasterly (winter) and southwesterly  
391 (summer). Thus, the major sources of aerosols were the Arabian Peninsula (including Saharan

392 dust and the Middle East) and Indian sub-continent in summer and winter respectively. The mean  
393 7-day back trajectory using HYSPLIT model from a point over the Arabian Sea (15N; 65E) was  
394 performed for each season of 2010 and at three different heights (500m, 1500m and 2500m  
395 above MSL). The Arabian Sea region was divided into four quadrants – 1) Arabian Peninsula and  
396 North Africa, 2) ~~Southern~~-Central Africa, 3) Indian sub-continent and 4) Indian Ocean and  
397 Southeast Asia (Fig. 54). ~~Similar to Table 2,~~The influence of different aerosol source regions  
398 over the Arabian Sea is given in Table 32.

399 Similar to Pease et al. (1998), Tindale and Pease (1999) found that transport of aerosols near  
400 the surface followed the surface wind currents. The dust content was low near the surface during  
401 summer due to the presence of Findlater jet, but the general dust concentrations were higher than  
402 other oceanic regions. During winter, the winds are predominantly north and northeasterly and  
403 hence results in transport of aerosols from India/Pakistan/Afghanistan onto the Arabian Sea.  
404 However, the presence of anticyclonic circulation over Arabia (20N; 60E) results in  
405 northwesterly winds transporting dust over the Arabian Sea (Rajeev et al., 2000). The springtime  
406 (March-April-May) is the transition between northeast and southwest monsoon. The winds  
407 become south westerlies which result in the advection of aerosols from the open Indian Ocean or  
408 near Somalia. At higher altitudes (above the Findlater jet) dust transport occurs from Arabia.  
409 During summer, the southwest monsoon wind patterns carry aerosols all the way from  
410 southeast/east Indian Ocean (mainly sea-salt). As the altitude increases, the wind patterns change  
411 a little due to aerosols coming from southwest Indian Ocean/Somalia. Above the Findlater jet, as  
412 explained by Tindale and Pease (1999), dust transport occurs from Arabian Peninsula (Table 32).

413 Being an integral part in the Indian Summer Monsoon, studies over the Bay of Bengal is  
414 important especially the role of aerosols in the local climate change. While the Arabian Sea is

415 dominated by dust and oceanic aerosols ~~and only anthropogenic aerosols during SON~~, studies  
416 have shown that the Bay of Bengal is influenced by various air masses associated with Asian  
417 monsoon system [including those of anthropogenic origin](#) (Krishnamurti et al., 1998). The  
418 synoptic meteorological conditions over the Bay of Bengal have been studied in detail by  
419 Moorthy et al. (2003) and Satheesh et al. (2006). Similar to the other two regions, mean 7-day  
420 back trajectory analysis from a point over (15N; 90N) was performed for each season of 2010  
421 and at three different heights (500m, 1500m and 2500m above MSL). The four quadrants  
422 representing the various aerosol source regions are 1) India/Arabian Peninsula, 2) Indian Ocean,  
423 3) North/Northeast India and East Asia and 4) Southeast Asia (Fig. [65](#)). Table [4-3](#) represents the  
424 influence of aerosol source regions over the Bay of Bengal.

425 The northwesterly winds occur from west to east in the Indo-Gangetic Plain (IGP) and due  
426 to subsidence, the aerosols are trapped in the east during winter (Dey and Di Girolamo, 2010; Di  
427 Girolamo et al., 2004). The IGP with its heavy population and large number of industries acts as  
428 a source for anthropogenic aerosols which are transported to Bay of Bengal during winter  
429 (Kumar et al., 2013). Along with mineral dust from the Arabian Peninsula, biomass aerosols  
430 from Southeast Asia are also transported to the bay. Field experiments like ICARB (Moorthy et  
431 al., 2008) during the springtime (pre-monsoon) showed transports of aerosols from the Arabian  
432 Peninsula and also the presence of elevated aerosols (anthropogenic and natural) over Bay of  
433 Bengal (Satheesh et al., 2008). The post-monsoon season acts as a transition from the summer to  
434 winter monsoon. The winds during September are still south westerlies and during October weak  
435 westerlies are present (Lawrence and Lelieveld, 2010). This results in transportation of aerosols  
436 from the Indian Ocean and the Arabian Sea. Thus, from Table [4-3](#) it can be seen that both  
437 anthropogenic aerosols (from IGP, Southeast Asia) and natural aerosols (marine and dust) are

438 present over the Bay of Bengal during different seasons.

### 439 **5.3. Role of Aerosol Layer Height in SSA retrieval**

440 Satheesh et al. (2009) devised a new algorithm to improve the retrieval of SSA using  
441 combined OMI and MODIS data. They used MODIS-predicted UV AOD as the input to improve  
442 the original OMI algorithm, which was constrained by the assumption of aerosol layer height.

443 Over the Atlantic, they found that on an average the AOD values retrieved from both algorithms  
444 ~~showed reasonably good agreement~~ agreed within  $\pm 0.1$ . However, over the Arabian Sea only  
445 when there was considerable loading of dust (especially during the March-April-May season),  
446 the OMI AOD and MODIS AOD had agreement suggesting that during other seasons, the  
447 assumption of aerosol height could be wrong. Satheesh et al. (2009) also found that over the  
448 Arabian Sea the aerosol layer height (ALH) derived from OMI-MODIS algorithm agreed well  
449 with aircraft measurements when compared to OMI SSA retrieval. In the current work, the  
450 aerosol layer height (ALH) ~~was calculated for~~ provide by OMI, ~~using the best estimate of SSA~~  
451 ~~retrieved from OMI~~ is the mean climatological height (section 2.1). For OMI-MODIS the ALH is  
452 estimated from OMI AOD values (at five different heights) by linear interpolation using AOD<sub>388</sub>  
453 as a reference (section 4). The difference in aerosol layer height (ALH) between OMI-MODIS  
454 and OMI was plotted against the difference in SSA over the Arabian Sea and Bay of Bengal (Fig.  
455 6a). The colorbar represents ALH estimated by OMI-MODIS algorithm. ~~The difference in~~  
456 ~~aerosol layer height between OMI-MODIS and OMI was plotted with the difference in SSA (Fig.~~  
457 ~~7a and 7b). The colorbar in the figure represents height estimated using the OMI-MODIS~~  
458 ~~algorithm.~~

459 The Mmost important observation from this analysis was that OMI overestimated SSA when  
460 it overestimated ALH (compared to OMI-MODIS) and vice versa. ~~OMI overestimates SSA at~~

461 ~~lower ALH (retrieved by OMI-MODIS algorithm) and underestimates SSA at higher ALH. The~~  
462 ~~latest version of OMI algorithm uses CALIPSO climatology of aerosol layer height for better~~  
463 ~~accuracy. However, over regions where this is not available, pre-defined aerosol height has been~~  
464 ~~used based on the type of aerosol assumed. For industrial sulphate aerosols exponential profile~~  
465 ~~with 2km scale height is assumed with a similar profile with 1.5km scale height for oceanic~~  
466 ~~aerosols. For biomass type aerosols, a Gaussian distribution with peak at 3km is used. Dust~~  
467 ~~aerosols are assumed to have two single Gaussian distributions with maximum at heights 3 and~~  
468 ~~5km.~~ It has been shown by Gassó and Torres (2016) that when the actual aerosol height  
469 measured by Satellite Lidar was 1.5km more than the climatological or assumed height, OMI  
470 retrieved higher SSA.

471 It can be seen from Figs. ~~76a and 7b~~, the blue coloured circles represent height estimated by  
472 OMI-MODIS between the surface to ~ 2km. In this range, it ~~is was~~ seen that the height assumed  
473 by OMI is > 1.5km compared to the one estimated by OMI-MODIS. Thus, OMI ~~overestimates~~  
474 overestimated SSA compared to the OMI-MODIS retrieval. ~~This overestimation is due to the~~  
475 ~~predefined vertical profiles. Thus, there are errors with regard to both the aerosol layer height as~~  
476 ~~well as the type of aerosol in the OMI algorithm. In the OMI algorithm, the highest uncertainty~~  
477 ~~in retrieving SSA is due to aerosol layer height and aerosol type (Torres et al., 2002). Using~~  
478 ~~ground based LIDAR measurements, Satheesh et al. (2009) concluded that OMI-MODIS~~  
479 ~~retrieved height agreed better with observations than OMI.~~

480 Gassó and Torres (2016), in their detailed analysis of the OMI UV aerosol product (version  
481 1.4.2), studied the OMI-MODIS method for two specific cases. They have mentioned that when  
482 the extrapolated MODIS 388nm AOD was not within the OMI LUT values, the OMI-MODIS  
483 algorithm retrieves unrealistic height and SSA. For the ARBOB region, the difference in AOD

484 ( $AOD_{MODIS} - AOD_{OMI}$ ) has been plotted with the difference in SSA ( $SSA_{OMI-MODIS} - SSA_{OMI}$ )  
485 (Fig. 6b). The colorbar represents the difference in ALH ( $ALH_{OMI-MODIS} - ALH_{OMI}$ ) retrieved by  
486 both the algorithms. An inverse relation was seen implying that when OMI underestimated AOD  
487 compared to MODIS, OMI overestimated SSA compared to OMI-MODIS. The difference in  
488 AOD was mainly within the  $\pm 0.5$  range. However, there are a few points where the AOD  
489 difference was  $> 3$ . Mostly in such cases, the difference between the ALH and SSA estimates of  
490 both the algorithms was high. However, there are points when the AOD difference was high and  
491 the ALH and SSA differences were within  $\pm 1$  km and  $\pm 0.03$  respectively. Similarly, the  
492 difference between ALH and SSA values of both the algorithms was high when the AOD  
493 difference was within  $\pm 0.5$ . These discrepancies could be attributed to the AOD spectral  
494 curvature of an aerosol type assumed by MODIS which is different by the aerosol model  
495 assumed by OMI UV aerosol product (Gassó and Torres, 2016). Whether any other property  
496 apart from AOD and shape (for dust aerosols) can affect the ALH and SSA retrievals have to be  
497 studied in the future.

498 The importance of ALH and SSA in the calculation of TOA flux ~~is~~ was studied using the  
499 Santa Barbara DISORT (SBDART) model (Ricchiazzi et al., 1998). For the same tropical  
500 environment variables and surface albedo of 0.06, the SSA was varied from 0.8 to 1 and aerosol  
501 height from 0 to 10 km at 1 km interval. The simulations were done for a narrow band in UV  
502 (300-400nm). For a constant AOD, AE (Angstrom Exponent) and asymmetry factor (0.4, 1 and  
503 0.7 respectively), TOA flux was calculated (Fig. 87a). It can be seen that at any ALH, TOA flux  
504 varied with SSA ~~in~~. The role of ALH is important in the UV region due to the phenomena of  
505 Rayleigh scattering (van de Hulst, 1981). The importance of Rayleigh scattering on the role of  
506 ALH is further shown in Fig. 97b. In this particular set of simulations, the Rayleigh scattering is

507 completely removed and all other parameters are kept the same as in Fig. 87a.

508 It can be seen that once molecular scattering is removed, the effect of ALH is also removed  
509 and TOA flux depends only on SSA and other aerosol properties. ~~This set of SBDART~~  
510 ~~simulations shows us how for a particular value of TOA flux, assuming different aerosol height~~  
511 ~~gives us different SSA values reiterating the important role of aerosol height on SSA~~  
512 ~~retrievals.~~The basis of many aerosol retrievals by satellites in the UV spectrum is the sensitivity  
513 of aerosol absorption to Rayleigh scattering which acts as a bright background and contributes to  
514 the TOA radiance (Torres et al., 1998; 2002). Change in ALH can affect the TOA radiance since  
515 the aerosol layer will interact with the Rayleigh scattering due to molecules present in the  
516 atmosphere. However, this effect is smaller compared to the effect due to the change in AOD and  
517 SSA (Kim et al., 2018). Kim et al. (2018) also showed how the misclassification of aerosol type  
518 and size could affect ALH retrieval. OMI SSA retrievals which are based on LUT depend on the  
519 ALH assumed along with aerosol type. The SBDART simulations in the current work show how  
520 for a particular TOA flux, SSA varies with ALH when the other aerosol properties are kept  
521 constant.

#### 522 **5.4. Validation** Comparison between SSA retrievals from OMI and OMI-MODIS with ship- 523 borne estimates.

524 To validate the new retrieval method of SSA using OMI and MODIS, both SSA values from  
525 OMI and OMI-MODIS were compared with ground-based measurements (SSA at 450nm)  
526 during ~~Cruises~~ cruises in the period 2006 and 2009 in the Arabian Sea and Bay of Bengal. These  
527 cruises were part of the Integrated Campaign for Aerosols, gases and Radiation Budget (ICARB)  
528 performed during the months of March to May 2006 and once during winter (W-ICARB) from  
529 27 December 2008 to 30 January 2009 (Moorthy et al., 2008 and 2010). During both the cruises



530 the aerosol sampling was done onboard the Oceanic Research Vessel *Sagar Kanya*. While the  
531 2006 cruise covered both the Arabian Sea and the Bay of Bengal, the winter cruise of 2009  
532 covered the Bay of Bengal. The cruise tracks are provided in detail in Moorthy et al., 2008 and  
533 2010, respectively. The SSA values at different wavelengths were estimated from spectral values  
534 of the absorption coefficient and scattering coefficient measured using the instruments  
535 Aethalometer (Magee Scientific AE-31, USA) and an integrating nephelometer (TSI 3563, USA)  
536 respectively. More details about the instrument and measuring techniques including the  
537 uncertainties are provided in Nair et al. (2008). However, both the cruise did not estimate SSA  
538 values in the UV spectrum. The closest wavelength at which SSA is calculated is 450nm which  
539 has been used to compare with the satellite retrievals of SSA (388nm). Ground-based SSA  
540 estimates based on in-situ measurements are seldom consistent with columnar satellite retrievals  
541 especially when elevated aerosols are present. This uncertainty along with the uncertainty in the  
542 assumption of SSA being uniform between 388nm and 450nm implies that the current  
543 comparison of study cannot be used as a validation study. Instead, it is used to understand the  
544 consistency of SSA retrievals from satellites with ground-based observations. ~~Since the spatial~~  
545 ~~coverage of OMI-MODIS and cruise measurements is less, the SSA values for both the~~  
546 ~~algorithms were averaged over the region of study and compared with observed SSA (Fig. 10).~~  
547 ~~However, the cruise measurements showed that SSA varied a lot spatially especially over Bay of~~  
548 ~~Bengal. Hence instead of a spatial average, the SSA values were temporally averaged for the~~  
549 ~~months when the cruise was performed. This was done under the assumption that during the~~  
550 ~~cruise period, the SSA over each location did not vary with time. For better coverage, a 1.5° box~~  
551 ~~was used around each location within which the mean SSA was calculated. Since the cruise~~  
552 measurements had little coverage spatially, for better coverage, a 2° box was used around each

553 location within which the mean SSA was calculated for the respective cruise period. These  
554 values are plotted in Fig. 8. OMI comparison is given by circles and OMI-MODIS by square  
555 markers. It can be seen that despite using a 2° box, the number of points having valid SSA values  
556 for the cruise and the satellite retrievals was only 21. This number increased as the size of the  
557 box around each cruise location was increased. The low number is due to the sparse nature of the  
558 OMI-MODIS retrieval over the region (Fig. 1b). The colour scale represents the cruise and the  
559 region where the aerosol sampling was taken.

560 During the ICARB, presence of elevated aerosols at a height of ~1km-3km have been shown  
561 in earlier studies (Satheesh et al., 2008; Nair et al., 2009). In such cases comparison between a  
562 ship-based aerosol retrieval which detects aerosols close to the surface and the SSA retrieval  
563 from satellites which detects these elevated aerosols cannot be considered appropriate. This  
564 discrepancy was seen in Fig. 8 especially over the Arabian Sea (Blue colour) and some points  
565 over Bay of Bengal (Red). In some cases, OMI was able to retrieve SSA consistent with the  
566 cruise estimated, unlike OMI-MODIS. This could be due to the improvement of dust model  
567 assumption in the new version of OMI aerosol product and (or) due to the wrong spectral AOD  
568 dependence assumed by MODIS. During the winter most of the aerosols influencing the Bay of  
569 Bengal is present closer to the surface. In such cases comparing the SSA estimates can be valid.  
570 It was observed that during winter when aerosols are generally present close to the surface, OMI-  
571 MODIS retrieved SSA which is a bit more consistent with the ship estimates compared to OMI.  
572 In such cases, OMI still overestimated SSA despite the improvement in the algorithm. The  
573 respective RMSEs for OMI and OMI-MODIS comparison with the cruise estimates were 0.05  
574 and 0.06. Due to the lack of common points, the correlation was also poor (OMI-MODIS: 0.11  
575 and OMI: -0.35).

576 The mean SSA of OMI, OMI-MODIS and cruise measurements are calculated and the  
577 difference between mean satellite SSA and mean SSA from cruise measurements are calculated  
578 for OMI and OMI-MODIS algorithms separately.

579 A statistical t test is performed comparing the respective SSA means of OMI and OMI-  
580 MODIS with SSA. The null hypothesis assumes the mean SSA of OMI/OMI-MODIS is equal to  
581 the mean SSA calculated from the cruise measurements. The values from Table 5 show that  
582 despite the mean difference of OMI SSA and cruise SSA being  $\sim 0.013$ , it was statistically  
583 significant at 95% significance level. On the other hand the SSA retrieved using OMI-MODIS  
584 algorithm was better constrained and was closer to the mean value of SSA from cruise  
585 measurements. The distribution of SSA from both the satellite algorithms as well as from cruise  
586 measurements is shown in Fig. 11.

587 Using five years (2008-2012) of OMI and OMI-MODIS data for the region of Arabian Sea  
588 and Bay of Bengal, SSA was retrieved and the difference between the two methods was  
589 calculated and plotted against SSA from the OMI-MODIS algorithm (Fig. 12). For absorbing  
590 aerosols detected by OMI-MODIS the SSA is overestimated by OMI.

591 The OMI-MODIS approach in SSA retrieval is one of the many combinations of sensors that  
592 can be used in retrieving aerosol properties. A ~~more complete~~better -approach involving ~~better~~  
593 the vertical distribution of aerosols either from space or ground-based observations is required to  
594 reduce the uncertainty further. However, with few ground-based measurements in the UV regime  
595 especially over the oceans and fewer retrievals of the vertical aerosol absorption, validation of  
596 new algorithms is still in the nascent stage.

## 597 6. Summary and Conclusions

598 Aerosol forcing depends on aerosol properties like aerosol optical depth (AOD) and single

599 scattering albedo (SSA). SSA is highly sensitive to the aerosol composition and size and as well  
600 as the wavelength at which the aerosol interacts with radiation. A slight change in SSA value can  
601 alter the sign of the forcing. Hence it is important to have an accurate measurement of SSA  
602 globally. [The](#) Ozone Monitoring Instrument (OMI) retrieves SSA in the UV spectrum. However,  
603 these retrievals are affected by cloud contamination and are sensitive to aerosol layer height. [In](#)  
604 [addition to these problems, uncertainty in the surface albedo is a source of error for SSA](#)  
605 [retrieval.](#) To resolve the issue of sub-pixel cloud contamination, Satheesh et al. (2009) developed  
606 a method using the combination of OMI and the Moderate Resolution Imaging  
607 Spectroradiometer (MODIS) at a local scale. In the present study, we used the method developed  
608 by Satheesh et al. (2009) to retrieve SSA at a much larger spatial and temporal scale. The main  
609 findings from our study are listed below:

- 610 1. Both OMI and OMI-MODIS algorithms retrieved SSA over regions influenced by large  
611 amounts of aerosols (e.g. Atlantic Ocean – ATL; Arabian Sea and Bay of Bengal –  
612 ARBOB)
- 613 2. ~~Difference in SSA retrievals of OMI-MODIS and OMI for both regions ATL and~~  
614 ~~ARBOB fluctuates between positive and negative values during different seasons which~~  
615 ~~could be due to the difference in either the type of aerosol or aerosol height assumed. In~~  
616 ~~addition, a longitudinal gradient of difference in SSA retrievals is present from the coast~~  
617 ~~of Sahara to the open ocean during the JJA season. This could be due the difference in~~  
618 ~~type of aerosols near the coast and in the open ocean~~[The difference in SSA retrievals of](#)  
619 [both the algorithms \( \$\Delta\$ SSA\) was found to be within  \$\pm 0.03\$  over ATL >80% of the time](#)  
620 [during all the seasons. Over the Arabian Sea, as seen in Satheesh et al. \(2009\),  \$\Delta\$ SSA was](#)  
621 [within the  \$\pm 0.03\$  range during MAM when the region was influenced by dust. The](#)

622 discrepancy during other season was due to the wrong assumption of aerosol layer height  
623 by OMI.

624 3. ~~OMI overestimates SSA at lower ALH and underestimates at higher values of ALH. Over~~  
625 ~~regions where CALIPSO climatology is not present, OMI uses pre-defined aerosol~~  
626 ~~heights based on the aerosol present. From Fig. 6a it was seen that OMI overestimated~~  
627 SSA when it overestimated ALH and vice versa. This could be attributed to the wrong  
628 assumption of aerosol height. Fig. 6b showed that difference in AOD and difference in  
629 SSA had an inverse relationship. Further analysis on whether any other factor apart from  
630 ALH and aerosol shape can affect SSA retrieval has to be studied.~~From Fig. 4 it is also~~  
631 ~~seen that OMI is unable to retrieve absorbing aerosols present at very low heights (<~~  
632 ~~2km) due to the already defined vertical profiles.~~

633 4. ~~In the UV spectrum, ALH plays a more dominant role than in the visible region due to~~  
634 ~~the major effect of Rayleigh scattering in UV. When Rayleigh scattering was removed,~~  
635 ~~ALH had no effect in both the UV and visible regions of the spectrum.~~

636 4. ~~OMI-MODIS method~~Both SSA retrievals ~~was validated using~~were compared with cruise  
637 data from the ICARB and W-ICARB campaigns in the Arabian Sea and Bay of Bengal.  
638 ~~The difference between OMI SSA and SSA from cruise measurements despite being~~  
639 ~~small is statistically significant. OMI-MODIS SSA is better constrained and is closer to~~  
640 ~~the cruise measurements~~

641 5. While both the algorithms did not match the cruise estimate during most of the dust  
642 season due to the presence of elevated aerosols, in few cases during ICARB, OMI  
643 performed better than OMI-MODIS. This could be due to the better assumption of dust  
644 model in the algorithm and/or wrong model assumption by MODIS. During winter, when

645 the aerosols were present closer to the surface, OMI-MODIS was a bit more consistent  
646 compared to OMI. This may be due to scenarios where the CALIPSO climatology was  
647 absent and OMI used its previous aerosol model assumptions. This could also be due to  
648 uncertainties in ALH value even after the improvement in the OMI algorithm with the  
649 addition of CALIPSO climatology.

650 ~~6. It is seen that the OMI overestimates SSA when absorbing aerosols were detected by~~  
651 ~~OMI-MODIS and the cruise measurements.~~

652 OMI retrieves aerosol properties at high cloud fraction (Gassó and Torres, 2016) implying  
653 two things, either OMI is able to detect aerosols present above clouds or the OMI pixel was  
654 prone to cloud contamination. In their study, Gassó and Torres (2016), observed that while  
655 MODIS cloud fraction could be used to screen out cloudy pixels in OMI, it could not be the lone  
656 criterion. While they performed for a single case, an analysis of a larger spatial and temporal  
657 scale is required. Aerosol type and aerosol layer height play a ~~very important~~vital role in the  
658 retrieval of aerosol properties. Without the assumption of aerosol type or height, OMI-MODIS ~~is~~  
659 ~~able to detect absorbing aerosols much better than OMI~~provided SSA retrievals which was  
660 consistent with cruise estimates during the winter when the Bay of Bengal was influenced by  
661 anthropogenic aerosols present close to the surface. This was not the case when dust aerosols  
662 were present. This discrepancy can be attributed to the difference in the aerosol model  
663 assumption by MODIS and OMI. This comparison study had very few points for a detailed  
664 analysis. ~~Hence this algorithm is useful over regions dominated by absorbing aerosols like Bay~~  
665 ~~of Bengal during winter. The importance of aerosol height is clearly demonstrated by SBDART~~  
666 ~~model and the validation with ground-based measurements highlighted the role of aerosol type.~~  
667 ~~However~~Hence, an accurate comparison and validation of such retrieval algorithms can be

668 possible only when there are more ground-based observations available in the UV spectrum on a  
669 larger spatial and temporal scale [along with vertical profiles of aerosol absorption](#).

## 670 **Acknowledgements**

671 The authors gratefully acknowledge the NOAA Air Resources Laboratory (ARL) for the  
672 provision of the HYSPLIT transport and dispersion model used in this publication. The authors  
673 are grateful to NASA data and services centre.

## 674 **References**

- 675 Bergstrom, R.W., Pilewskie, P., Russell, P.B., Redemann, J., Bond, T.C., Quinn, P.K., and Sierau,  
676 B.: Spectral absorption properties of atmospheric aerosols, *Atmos. Chem. Phys.*, 7, 5937-  
677 5943, 2007.
- 678 Bond, T.C., and Sun, H.: Can reducing black carbon emissions counteract global warming?,  
679 *Environ. Sci. Technol.*, 39(16), 5921-5926, 2005.
- 680 Bond, T.C., and Bergstrom, R.W.: Light absorption by carbonaceous particles: An investigative  
681 review, *Aerosol Sci. Tech.*, 40(1), 27-67, doi:10.1080/02786820500421521, 2006.
- 682 Bond, T.C., Doherty, S.J., Fahey, D.W., Forster, P.M., Bernsten, T., De Angelo, B.J., Flanner,  
683 M.G., Ghan, S., Karcher, B., Koch, D., Kinne, S., Kondo, Y., Quinn, P.K., Sarofim, M.C.,  
684 Schultz, M., Venkataraman, C., Zhang, H., Zhang, S., Bellouin, N., Guttikunda, S.K.,  
685 Hopke, P.K., Jacobson, M.Z., Kaiser, J.W., Klimont, Z., Lohmann, U., Schwarz, J.P.,  
686 Shindell, D., Storelvmo, T., Warren, S.G., and Zender, C.S.: Bounding the role of black  
687 carbon in the climate system: A scientific assessment, *J. Geophys. Res.*, 118(11), 5380-  
688 5552, doi:10.1002/jgrd.50171, 2013.
- 689 Chand, D., Wood, R., Anderson, T.L., Satheesh, S.K., and Charlson, R.J.: Satellite-derived direct  
690 radiative effect of aerosols dependent on cloud cover, *Nat. Geosci.*, 2, 181–184,

691 doi:10.1038/ngeo437, 2009.

692 Chung, S.H., and Seinfeld, J.H.: Global distribution and climate forcing of carbonaceous  
693 aerosols, *J. Geophys. Res.*, 107(D19), 4407, doi:10.1029/2001JD001397, 2002.

694 Cooke, W.F., and Wilson, J.J.N.: A global black carbon aerosol model, *J. Geophys. Res.*, 101,  
695 19395-19410, doi:10.1029/96JD00671, 1996.

696 Dey, S., and Di Girolamo, L.: A climatology of aerosol optical and microphysical properties over  
697 the Indian subcontinent from 9 years (2000–2008) of Multiangle Imaging  
698 Spectroradiometer (MISR) data, *J. Geophys. Res.*, 115, D15204,  
699 doi:10.1029/2009JD013395, 2010.

700 Di Girolamo, L., Bond, T.C., Bramer, D., Diner, D.J., Fettingner, F., Kahn, R.A., Mrtonchik, J.V.,  
701 Ramana, M.V., Ramanathan, V., and Rasch, P.J.: Analysis of Multi-angle Imaging  
702 SpectroRadiometer (MISR) aerosol optical depths over greater India during winter 2001-  
703 2004, *Geophys. Res. Lett.*, 31(23), L23115, doi:10.1029/2004GL021273, 2004.

704 Diner, D.J., Beckert, J.C., Reilly, T.H., Bruegge, C.J., Conel, J.E., Kahn, R.A., Martonchik, J.V.,  
705 Ackerman, T.P., Davies, R., Gerstl, S.A.W., Gordon, H.R., Muller, J.-P., Myneni, R.B.,  
706 Sellers, P.J., Pinty, B., and Verstraete, M.M.: Multi-angle Imaging SpectroRadiometer  
707 (MISR) instrument description and experiment overview, *IEEE T GEOSCI REMOTE*,  
708 36(4), 1072-1087, doi:10.1109/36.700992, 1998.

709 Dubovik, O., and King, M.D.: A flexible inversion algorithm for retrieval of aerosol optical  
710 properties from Sun and sky radiance measurements, *J. Geophys. Res.*, 105(D16), 20673-  
711 20696, doi:10.1029/2000JD900282, 2000.

712 Dubovik, O., Holben, B.N., Eck, F.T., Smirnov, A., Kaufman, Y.J., King, M.D., ~~Tanre~~Tanré, D.,  
713 and Slutsker, I.: Variability of absorption and optical properties of key aerosol types



714 observed in worldwide locations, *J. Atmos. Sci.*, 59(3), 590-608, doi:10.1175/1520-  
715 0469(2002)059<0590:VOAAOP>2.0.CO;2, 2002.

716 Eck, T.F., Holben, B.N., Slutsker, I., and Setzer, A.: Measurements of irradiance attenuation and  
717 estimation of aerosol single scattering albedo for biomass burning aerosols in Amazonia, *J.*  
718 *Geophys. Res.*, 103(D24), 31865-31878, doi:10.1029/98JD00399, 1998.

719 Gassó, S., and Torres, O.: The role of cloud contamination, aerosol layer height and aerosol  
720 model in the assessment of the OMI near-UV retrievals over the ocean, *Atmos. Meas.*  
721 *Tech.*, 9, 3031-3052, doi:10.5194/amt-9-3031-2016, 2016.

722 Hansen, J., Sato, M., and Ruedy, R.: Radiative forcing and climate response, *J. Geophys. Res.-*  
723 *Atmos.*, 102(D6), 6831-6864, doi:10.1029/96JD03436, 1997.

724 Harriss, R.C., Browell, E.V., Sebacher, D.I., Gregory, G.L., Hinton, R.R., Beck, S.M., McDougal,  
725 D.S., and Shipley, S.T.: Atmospheric transport of pollutants from North America to the  
726 North Atlantic Ocean, *Nature*, 308, 722-724, doi:10.1038/308722a0, 1984.

727 Haywood, J.M., Roberts, D.L., Slingo, A., Edwards, J.M., and Shine, K.P.: General circulation  
728 model calculations of the direct radiative forcing by anthropogenic sulphate and fossil-fuel  
729 soot aerosol, *J. Clim.*, 10, 1562-1577, doi:10.1175/1520-  
730 0442(1997)010<1562:GCMCOT>2.0.CO;2, 1997.

731 Heintzenberg, J., Charlson, R.J., Clarke, A. D., Liousse, C., Ramaswamy, V., Shine, K.P.,  
732 Wendish, M., and Helas, G.: Measurements and modelling of aerosol single-scattering  
733 albedo: Progress, problems and prospects, *Contrib. Atmos. Phys.*, 70(4), 249– 263, 1997.

734 Herman, B.M., Browning, R.S., and De Luisi, J.J.: Determination of the effective imaginary term  
735 of the complex refractive index of atmospheric dust by remote sensing: the diffuse-direct  
736 radiation method, *J. Atmos. Sci.*, 32, 918-925, doi:10.1175/1520-

737 0469(1975)032<0918:DOITEIT>2.0.CO;2, 1975.

738 Herman, J.R., Bhartia, P.K., Torres, O., Hsu, C., Seftor, C., and Celarier, E.: Global distribution  
739 of UV-absorbing aerosols from Nimbus 7/TOMS data, *J. Geophys. Res.-Atmos.*, 102(D14),  
740 16911-16922, doi:10.1029/96JD03680, 1997.

741 Horvath, H.: Atmospheric light absorption- a review, *Atmos. Environ. A-Gen.*, 27(3), 293-317,  
742 doi:10.1016/0960-1686(93)90104-7, 1993.

743 Intergovernmental Panel on Climate Change (IPCC) (2013), The physical science basis:  
744 Contribution of Working Group I to the Fifth Assessment Report of the Intergovernmental  
745 Panel on Climate Change, In: *Climate Change (2013)*, Stocker, T.F., D. Qin, G.K. Plattner,  
746 M. Tignor, S.K. Allen, J. Boschung, A. Nauels, Y. Xia, V. Bex, and P.M. Midgley (eds),  
747 Cambridge University, Press: Cambridge, United Kingdom and New York, NY, USA 1535  
748 pp, doi:10.1017/CBO9781107415324.

749 Jethva, H., Torres O., and Ahn C.: Global assessment of OMI aerosol single-scattering albedo  
750 using ground-based AERONET inversion, *J. Geophys. Res.-Atmos.*, 119(14), 9020-9040,  
751 doi:10.1002/2014JD021672, 2014.

752 Johnson, B.T., Shine, K.P., and Forster, P.M.: The semi-direct aerosol effect: Impact of absorbing  
753 aerosols on marine stratocumulus, *Q. J. Roy. Meteor. Soc.*, 130, 1407-1422,  
754 doi:10.1256/qj.03.61, 2003.

755 Kaufman, Y.J.: Satellite sensing of aerosol absorption, *J. Geophys. Res.*, 92, 4307-4317,  
756 doi:10.1029/JD092iD04p04307, 1987.

757 Kaufman, Y.J., ~~Fanre~~ Tanré, D., and Boucher, O.: A satellite view of aerosols in the climate  
758 system, *Nature*, 419, 215-223, doi:10.1038/nature01091, 2002a.

759 Kaufman, Y.J., Martins, J.V., Remer, L.A., Schoeberl, M.R., and Yamasoe, M.A.: Satellite

760 retrieval of aerosol absorption over the oceans using sunglint, *Geophys. Res. Lett.*, 29(19),  
761 34-1 – 34-4, doi:10.1029/2002GL015403, 2002b.

762 Kaufman, Y.J., Koren, I., Remer, L.A., ~~Tanre~~[Tanré](#), D., Ginoux, P., and Fan, S.: Dust transport  
763 and deposition observed from the Terra-Moderate Resolution Imaging Spectroradiometer  
764 (MODIS) spacecraft over the Atlantic Ocean, *J. Geophys. Res.*, 110, D10S12,  
765 doi:10.1029/2003JD004436, 2005.

766 Kim, S-W., Yoon, S-C., Jefferson, A., Won, J-G, Dutton, E.G, Ogren, J.A., and Anderson T.L.:  
767 Observation of enhanced water vapour in Asian dust layer and its effect on atmospheric  
768 radiative heating rates, *Geophys. Res. Lett.*, 31(18), doi:10.1029/2004GL020024, 2004.

769 [Kim, M., Kim, J., Torres, O., Ahn, C., Kim, W., Jeong, U., Go, S., Liu X., Moon, K.J., and Kim,  
770 D.-R.: Optimal Estimation-Based Algorithm to Retrieve Aerosol Optical Properties for  
771 GEMS Measurements over Asia, \*Remote Sens.\*, 10\(2\), 162, doi:10.3390/rs10020162, 2018.](#)

772 King, M.D.: Determination of the ground albedo and the index of absorption of atmospheric  
773 particulates by remote sensing. Part II: Application, *J. Atmos. Sci.*, 36, 1072-1083,  
774 doi:10.1175/1520-0469(1979)036<1072:DOTGAA>2.0.CO;2, 1979.

775 Krishnamurti, T.N., Jha, B., Prospero J., Jayaraman, A., and Ramanathan, V.: Aerosol and  
776 pollutant transport and their impact on radiative forcing over the tropical Indian Ocean  
777 during the January – February 1996 pre-INDOEX cruise, *Tellus B*, 50(5): 521–542,  
778 doi:10.1034/j.1600-0889.1998.00009.x, 1998.

779 Kumar, K.R., Sivakumar, Reddy, R.R., and Gopal, K.R.: Ship-borne measurements of columnar  
780 and surface aerosol loading over the Bay of Bengal during W-ICARB campaign: role of  
781 airmass transport. Latitudinal and Longitudinal Gradients, *Aerosol Air Qual Res.*, 13, 818–  
782 837, doi:10.4209/aaqr.2012.08.0225, 2013.

783 Lawrence, M.G., and Lelieveld, J.: Atmospheric pollutant outflow from southern Asia: a review,  
784 Atmospheric Chemistry and Physics, 10, 11017-11096, doi:10.5194/acp-10-11017-2010,  
785 2010.

786 Levy, R.C., Remer, L.A., ~~Fanre~~Tanré, D., Kaufman, Y.J., Ichoku, C., Holben, B.N., Livingston,  
787 J.M., Russell, P.B., and Maring, H.: Evaluation of the Moderate-Resolution Imaging  
788 Spectroradiometer (MODIS) retrievals of dust aerosol over the ocean during PRIDE, J.  
789 Geophys. Res., 108(D19), 8594, doi:10.1029/2002JD002460, 2003.

790 Liao, H., and Seinfeld, J.H.: Radiative forcing by mineral dust aerosols: Sensitivity to key  
791 variables, J. Geophys. Res.-Atmos., 103(D24), 31637-31645, doi:10.1029/1998JD200036,  
792 1998.

793 Meloni, D., di Sarra, A., di Lorio, T., and Fiocco, G.: Influence of the vertical profile of Saharan  
794 dust on the visible direct radiative forcing, J. Quant. Spectrosc. Ra., 93(4), 397-413,  
795 doi:10.1016/j.jqsrt.2004.08.035, 2005.

796 Menon, S., Hansen, J., Nazarenko, L., and Luo, Y.: Climate effects of black carbon aerosols in  
797 China and India, Science, 297(5590), 2250-2253, doi:10.1126/science.1075159, 2002.

798 Mishra, A.K., Koren, I., and Rudich, Y.: Effect of aerosol vertical distribution on aerosol-  
799 radiation interaction: A theoretical prospect, Heliyon, e00036,  
800 doi:10.1016/j.heliyon.2015.e00036, 2015.

801 Moorthy, K.K., Babu, S.S., and Satheesh, S.K.: Aerosol spectral optical depths over the Bay of  
802 Bengal: role of transport, Geophys. Res. Lett., 30(5): 1249, doi:10.1029/2002GL016520,  
803 2003.

804 Moorthy, K.K., Babu, S.S., Sunilkumar, S.V., Gupta, P.K., and Gera, B.S.: Altitude profiles of  
805 aerosol BC, derived from aircraft measurements over an inland urban location in India,

806 Geophys. Res. Lett., 31(22), 10.1029/2004GL021336, 2004.

807 Moorthy, K.K., Satheesh, S.K., Babu, S.S., and Dutt, C.B.S.: Integrated campaign for aerosols,  
808 gases and radiation budget (ICARB): an overview, *J. Earth. Syst. Sci.*, 117(1), 243-262,  
809 doi:10.1007/s12040-008-0029-7, 2008.

810 Moorthy, K.K., Beegum, S.N., Babu, S.S., Smirnov, A., John, S.R., Kumar, K.R., Narasimhulu,  
811 K., Dutt, C.B.S., and Nair, V.S.: Optical and physical characteristics of Bay of Bengal  
812 aerosols during W-ICARB: spatial and vertical heterogeneities in the marine atmospheric  
813 boundary layer and in the vertical column, *J. Geophys. Res.*, 115(D24): D24213,  
814 doi:10.1029/2010JD014094, 2010.

815 Moosmuller, H., Chakrabarty, R.K., and Arnott, W.P.: Aerosol light absorption and its  
816 measurement: A review, *J. Quant. Spectrosc. Ra.*, 110(11), 844-878,  
817 doi:10.1016/j.jqsrt.2009.02.035, 2009.

818 Morris, V., Colon, P.C., Nalli, N.R., Joseph, E., Armstrong, R.A., Detres, Y., Goldberg, M.D.,  
819 Minnett, P.J., and Lumpkin, R.: Measuring Trans-Atlantic aerosol transport from Africa,  
820 *EOS Trans. AGU*, 87(50), 565-571, doi:10.1029/2006EO500001, 2006.

821 Myhre, G., Stordal, F., Restad, K., and Isaksen, I.S.A.: Estimation of the direct radiative forcing  
822 due to sulphate and soot aerosols, *Tellus*, 50B, 463-477, 1998.

823 [Nair, V.S., Babu, S.S., and Moorthy, K.K.: Spatial distribution and spectral characteristics of](#)  
824 [aerosol single scattering albedo over the Bay of Bengal inferred from shipborne](#)  
825 [measurements, \*Geophys. Res. Lett.\*, 35, doi:10.1029/2008GL033687, 2008.](#)

826 [Nair V.S., Moorthy, K.K., and Babu, S.S.: Optical and Physical Properties of Atmospheric](#)  
827 [Aerosols over the Bay of Bengal during ICARB, \*J. Atmos. Sci.\*, 66, doi:](#)  
828 [10.1175/2009JAS3032.1, 2009.](#)

829 Narasimhan, D., and Satheesh, S.K.: Estimates of aerosol absorption over India using multi-  
830 satellite retrieval, *Ann. Geophys.*, 31, 1773-1778, doi:10.5194/angeo-31-1773-2013, 2013.

831 Pease, P.P., Tchakerian, V.P., and Tindale, N.W.: Aerosols over the Arabian Sea: geochemistry  
832 and source areas for Aeolian desert dust, *J. Arid Environ.*, 39(3), 477-496,  
833 doi:10.1006/jare.1997.0368, 1998.

834 Podgorny, I.A., and Ramanathan, V.: A modeling study of the direct effect of aerosols over the  
835 tropical Indian Ocean, *J. Geophys. Res.*, 106(D20): 24097–24105,  
836 doi:10.1029/2001JD900214, 2001.

837 Prospero, J.M., and Carlson, T.N.: Vertical and areal distribution of Saharan dust over the  
838 western equatorial north Atlantic Ocean, *J. Geophys. Res.*, 77(27), 5255-5265,  
839 doi:10.1029/JC077i027p05255, 1972.

840 Prospero, J.M.: Saharan dust transport over the North Atlantic Ocean and Mediterranean: An  
841 overview, In: *The Impact of Desert Dust Across the Mediterranean*, Guerzoni S., Chester  
842 R. (Eds.), 133-151, doi:10.1007/978-94-017-3354-0\_13, 1996.

843 Rajeev, K., Ramanathan, V., and Meywerk, J.: Regional aerosol distribution and its long-range  
844 transport over the Indian Ocean, *J. Geophys. Res.-Atmos.*, 105(D2), 2029-2043,  
845 doi:10.1029/1999JD900414, 2000.

846 Ramanathan, V., Crutzen, P.J., Kiehl, J.T., and Rosenfield, D.: Aerosols, climate and the  
847 hydrological cycle, *Science*, 294(5549): 2119–2124, doi:10.1126/science.1064034, 2001.

848 Remer, L. A., Kaufman, Y. J., ~~Fanre~~ Tanré, D., Mattoo, S., Chu, D. A., Martins, J. V., Li, R. R.,  
849 Ichoku, C., Levy, R. C., Kleidman, R. G., Eck, T. F., Vermote, E., and Holben, B. N.: The  
850 MODIS aerosol algorithm, products, and validation, *J. Atmos. Sci.*, 62, 947–973,  
851 doi:10.1175/JAS3385.1, 2005.

852 Ricchiazzi, P., Yang, S., Gautier, C., and Sowle, D.: SBDART: a research and teaching software  
853 tool for plane-parallel radiative transfer in the earth's atmosphere, *B. Am. Meteorol. Soc.*  
854 79(10): 2101–2114, doi:10.1175/1520-0477(1998)079<2101: SARATS>2.0.CO;2, 1998.

855 Satheesh, S.K.: Aerosols and climate, *Resonance*, 7(4), 48-59, doi:10.1007/BF02836138, 2002.

856 Satheesh, S.K., and Moorthy, K.K.: Radiative effects of natural aerosols: a review, *Atmos.*  
857 *Environ.*, 39(11): 2089–2110, doi:10.1016/j.atmosenv.2004.12.029, 2005.

858 Satheesh, S.K., Srinivasan, J., and Moorthy, K.K.: Spatial and temporal heterogeneity in aerosol  
859 properties and radiative forcing over Bay of Bengal: Sources and role of aerosol transport,  
860 *J. Geophys. Res.*, 111(D8): D08202, doi:10.1029/2005JD006374, 2006.

861 Satheesh, S.K., Moorthy, K.K., Babu, S.S., Vinoj, V., and Dutt, C.B.S.: Climate implications of  
862 large warming by elevated aerosol over India, *Geophys. Res. Lett.*, 35(19),  
863 doi:10.1029/2008GL034944, 2008.

864 Satheesh, S.K., Torres, O., Remer, L.A., Babu, S.S., Vinoj, V., Eck, T.F., Kleidman, R.G., and  
865 Holben, B.N.: Improved assessment of aerosol absorption using OMI-MODIS joint  
866 retrieval, *J. Geophys. Res.*, 114, D05209, doi:10.1029/2008JD011024, 2009.

867 Satheesh, S.K., Vinoj, V., and Moorthy, K.K.: Assessment of aerosol radiative impact over  
868 oceanic regions adjacent to Indian subcontinent using multi-satellite analysis, *Adv.*  
869 *Meteorol.*, 2010, Article ID 139186, pp 13., doi:10.1155/2010/139186, 2010.

870 Seinfeld, J.H., and Pandis, S.N.: *Atmospheric Chemistry and Physics: From air pollution to*  
871 *climate change*, 2nd Ed., 1232 pp, John Wiley & Sons, Inc., Hobkoben, New Jersey, 2006.

872 Sirocko, F., and Sarnthein, M.: Wind-borne deposits in the northwestern Indian Ocean: Record of  
873 Holocene sediments versus modern satellite data, In: *Paleoclimatology and*  
874 *Paleometeorology: modern and past patterns of global atmospheric transport*, Leinen M.,

875 Sarnthein M. (Eds), 401-433, Amsterdam: Kluwer Academic Publishers, 1989.

876 Stephens, G.L., Vane, D.G., Boain, R.J., Mace, G.G., Sassen, K., Wang, Z., Illingworth, A.J.,  
877 O'Connor, E.J., Rossow, W.B., Durden, S.L., Miller, S.D., Austin, R.T., Benedetti, A.,  
878 Mitrescu, C., and CloudSat Science Team: The CloudSat mission and the A-Train: A new  
879 dimension of space-based observations of clouds, precipitation, B. Am. Meteorol. Soc., 83,  
880 1771-1790, doi:10.1175/BAMS-83-12-1771, 2002.

881 ~~Tanre~~Tanré, D., Kaufman, Y.J., Herman, M., and Mattoo, S.: Remote sensing of aerosol  
882 properties over oceans using the MODIS/EOS spectral radiances, J. Geophys. Res.,  
883 102(D14), 16971–16988, 1997.

884 Tindale, N.W., and Pease, P.P.: Aerosols over the Arabian Sea: Atmospheric transport pathways  
885 and concentrations of dust and sea salt, Deep-Sea Res. Pt. II, 46(8-9), 1577-1595,  
886 doi:10.1016/S0967-0645(99)00036-3, 1999.

887 Torres, O., Bhartia, P. K., Herman, J. R., and Ahmad, Z.: Derivation of aerosol properties from  
888 satellite measurements of backscattered ultraviolet radiation. Theoretical Basis, J.  
889 Geophys. Res., 103(D14), 17099–17110, 1998.

890 Torres, O., Decae, R., Veefkind, J.P., and de Leeuw, G.: OMI aerosol retrieval algorithm, in OMI  
891 Algorithm Theoretical Basis Document: Clouds, Aerosols, and Surface UV Irradiance, 3,  
892 V2, OMIATBD- 03, edited by P. Stammes, pp. 47 – 71, NASA Goddard Space Flight  
893 Cent., Greenbelt, Md, 2002.  
894 ([http://eosps0.gsfc.nasa.gov/eos\\_homepage/for\\_scientists/atbd/docs/OMI/ATBD-OMI-](http://eosps0.gsfc.nasa.gov/eos_homepage/for_scientists/atbd/docs/OMI/ATBD-OMI-03.pdf)  
895 [03.pdf](http://eosps0.gsfc.nasa.gov/eos_homepage/for_scientists/atbd/docs/OMI/ATBD-OMI-03.pdf))

896 Torres, O., Bhartia, P.K., Sinyuk, A., Welton, E.J., and Holben, B.: Total Ozone Mapping  
897 Spectrometer measurements of aerosol absorption from space: Comparison to SAFARI



898 2000 ground-based observations, *J. Geophys. Res.*, 110(D10), doi:10.1029/2004JD004611,  
899 2005.

900 Torres, O., Tanskanen, A., Veihelmann, B., Ahn, C., Braak, R., Bhartia, P.K., Veefkind, P., and  
901 Levelt, P.: Aerosols and surface UV products from Ozone Monitoring Instrument  
902 observations: An overview, *J. Geophys. Res.*, 112, D24S47, doi:10.1029/2007JD008809,  
903 2007.

904 Torres, O., Ahn, C., and Chen, Z.: Improvements to the OMI near-UV aerosol algorithm using A-  
905 train CALIOP and AIRS observations, *Atmos. Meas. Tech.*, 6, 3257-3270,  
906 doi:10.5194/amt-6-3257-2013, 2013.

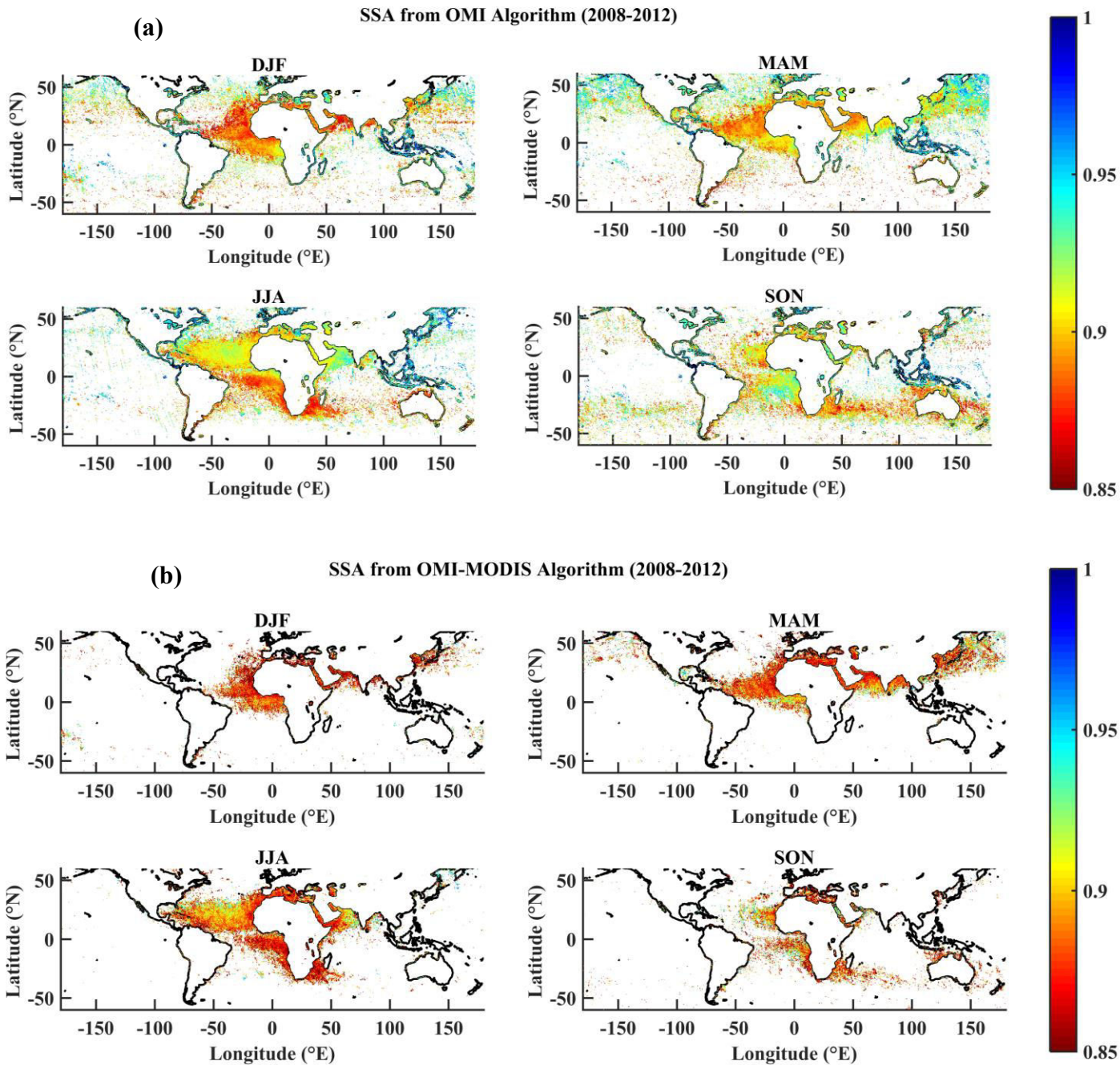
907 [Torres, O., Bhartia, P.K., Jethva, H., and Ahn, C.: Impact of the ozone monitoring instrument row](#)  
908 [anomaly on the long-term record of aerosol products, \*Atmos. Meas. Tech.\*, 11, 2701-2715,](#)  
909 [doi:10.5194/amt-11-2701-2018, 2018.](#)

910 Van de Hulst, H.C.: Light scattering by small particles, 496 pp., Dover publications, New York,  
911 1981.

912 Wells, K.C., Martins, J.V., Remer, L.A., Kreidenweis, S.M., and Stephens, G.L.: Critical  
913 reflectance derived from MODIS: Application for the retrieval of aerosol absorption over  
914 desert regions, *J. Geophys. Res.*, 117(D3), doi:10.1029/2011JD016891, 2012.

915 Zhu, L., Martins, J.V., and Remer, L.A.: Biomass burning aerosol absorption measurements with  
916 MODIS using the critical reflectance method, *J. Geophys. Res.*, 116(D7),  
917 doi:10.1029/2010JD015187, 2011.

918 Zuluaga, M.D., Webster, P.J., and Hoyos, C.D.: Variability of aerosols in the tropical Atlantic  
919 Ocean relative to African Easterly Waves and their relationship with atmospheric and  
920 oceanic environments, *J. Geophys. Res.*, 117(D16), doi:10.1029/2011JD017181, 2012.

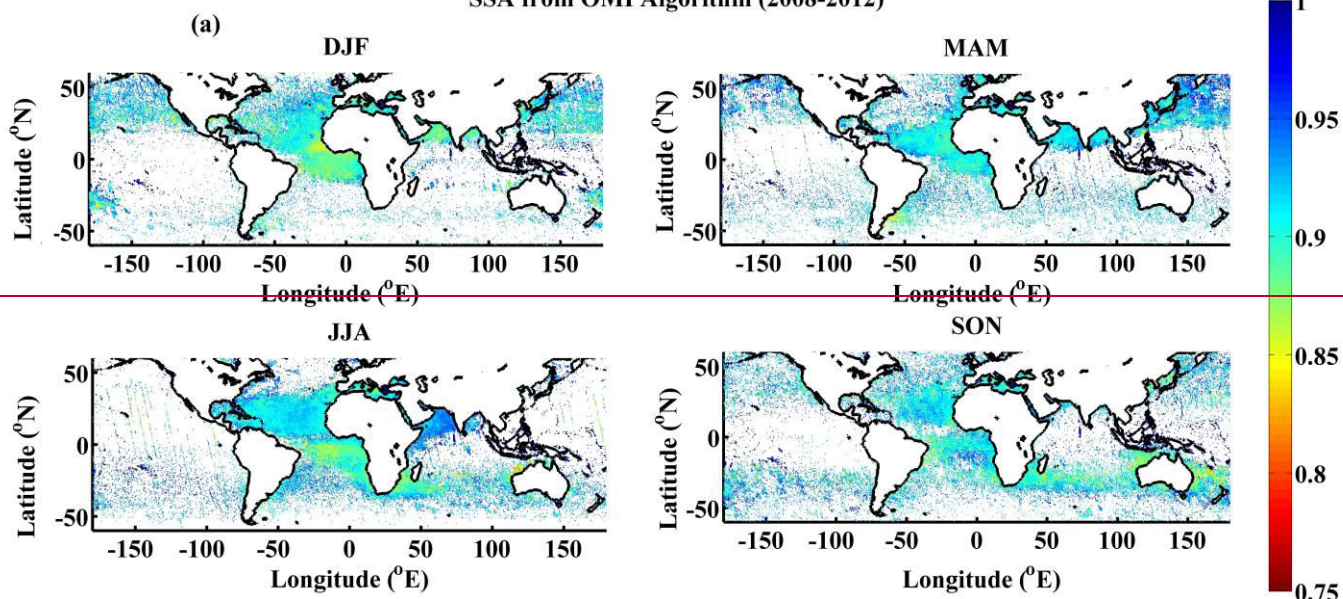


921

922

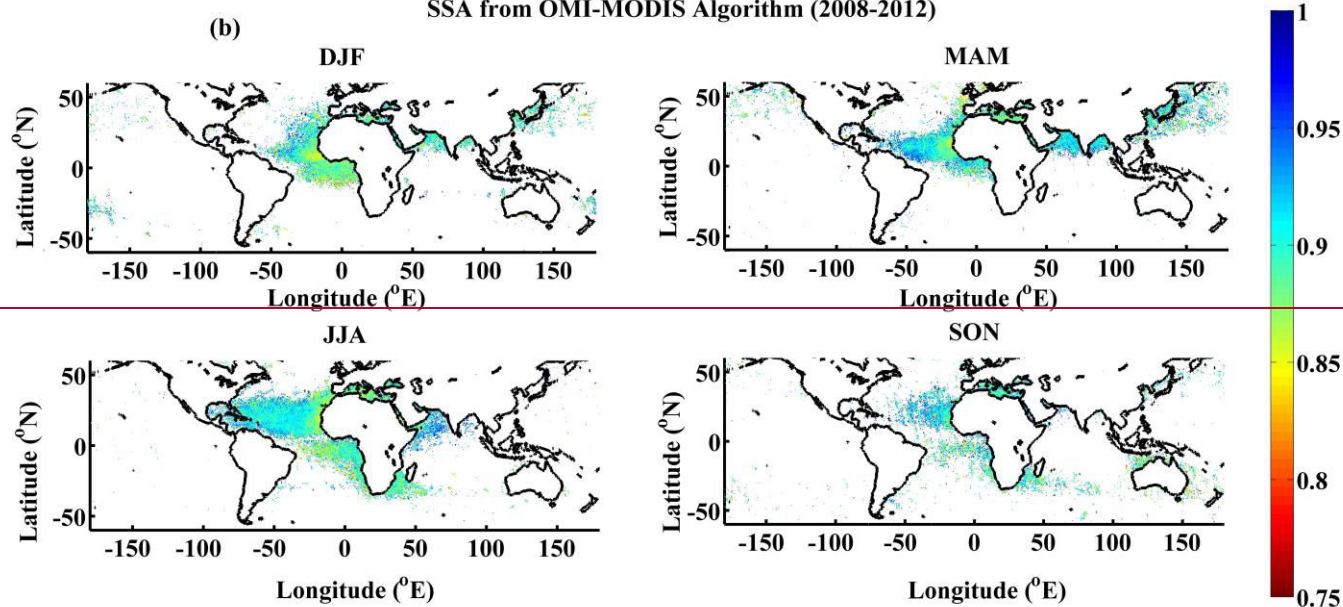
923 **Figure 1b.** Spatial distribution of SSA at 388nm retrieved by a) OMI and b) OMI-MODIS. In the  
 924 present study, points which had the same SSA value at the 5 discrete heights provided by OMI or  
 925 an invalid value at any one height were considered invalid for the OMI-MODIS retrieval since  
 926 interpolation was not possible. This resulted in the reduction of the number of valid points for  
 927 OMI-MODIS when compared to OMI.

SSA from OMI Algorithm (2008-2012)



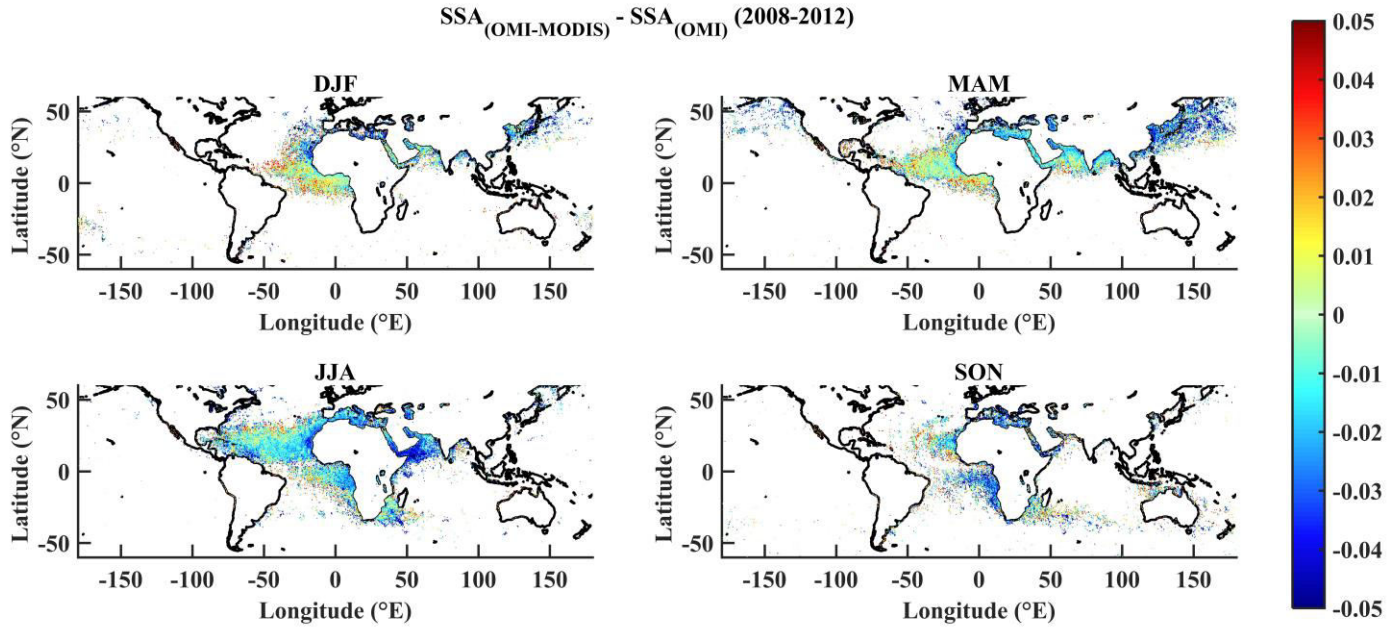
928

SSA from OMI-MODIS Algorithm (2008-2012)



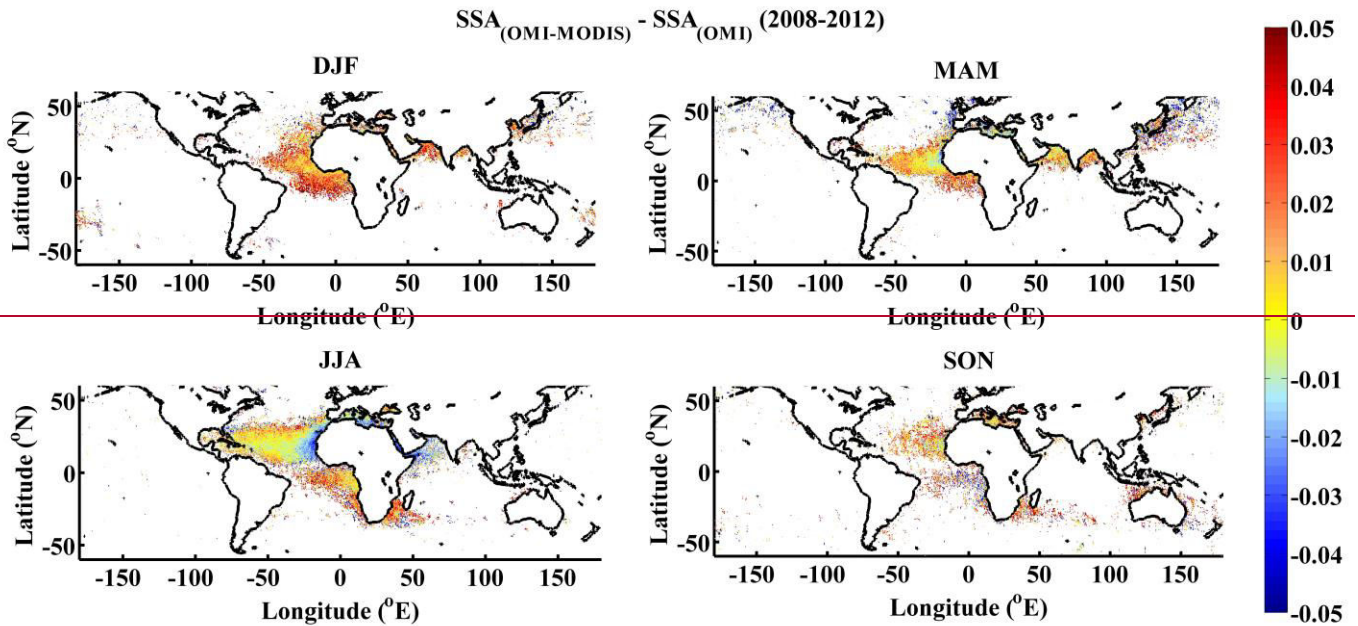
929





930

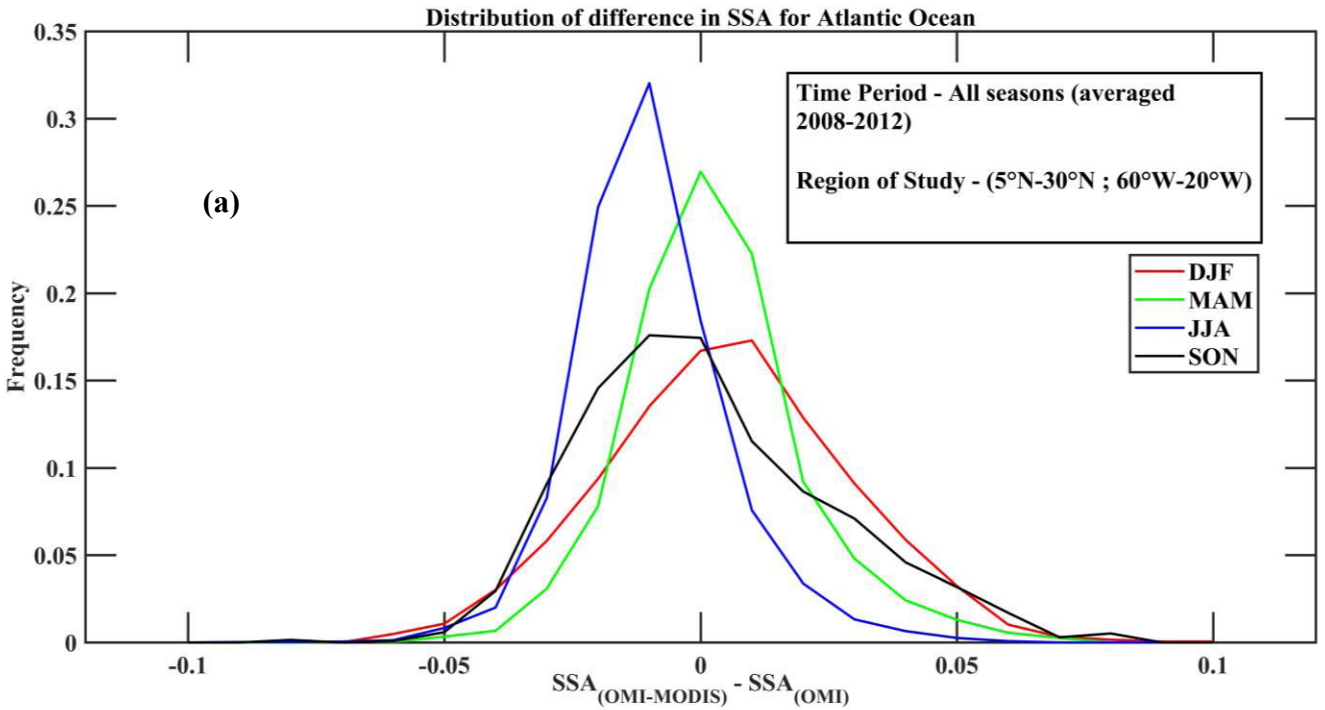
931 **Figure 2.** Spatial distribution of difference in SSA [retrieved by OMI-MODIS](#) and SSA [retrieved](#)  
 932 [by OMI, both at 388nm. retrievals](#)When the OMI-MODIS SSA value was found invalid, the  
 933 [difference was also considered to be invalid.](#)



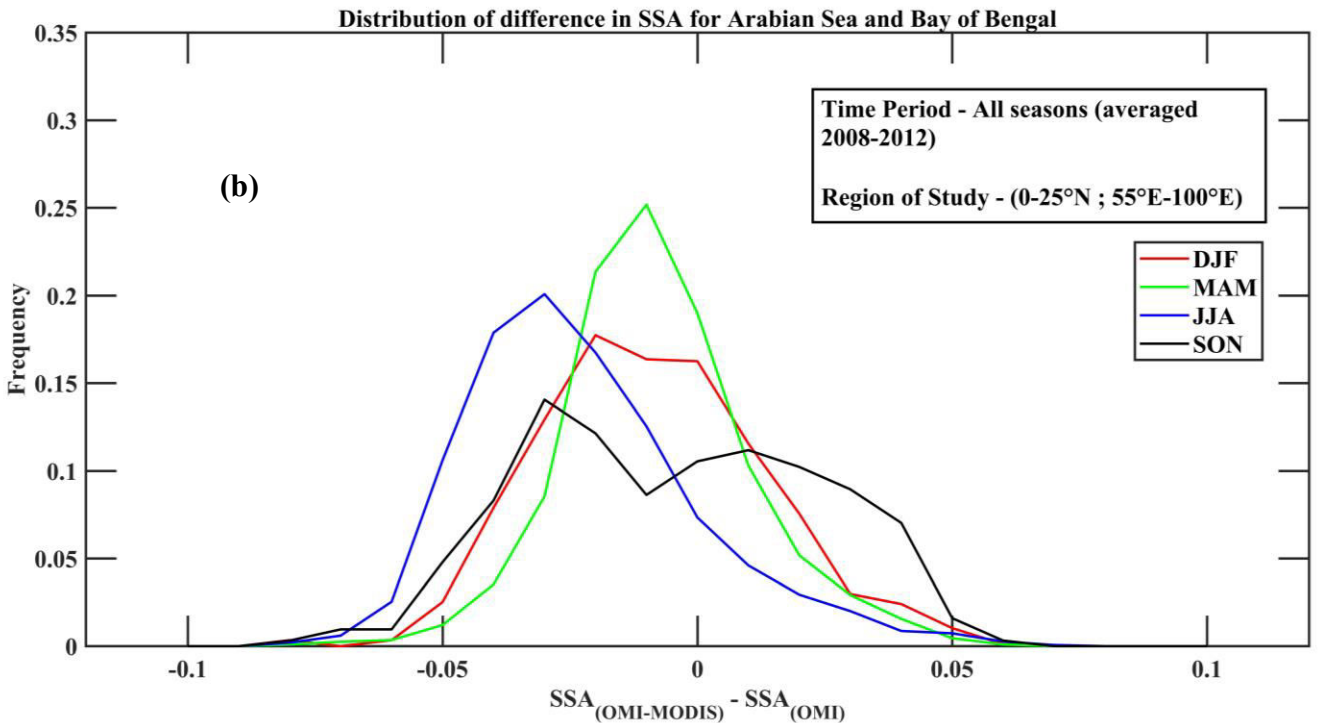
934

935

936



937

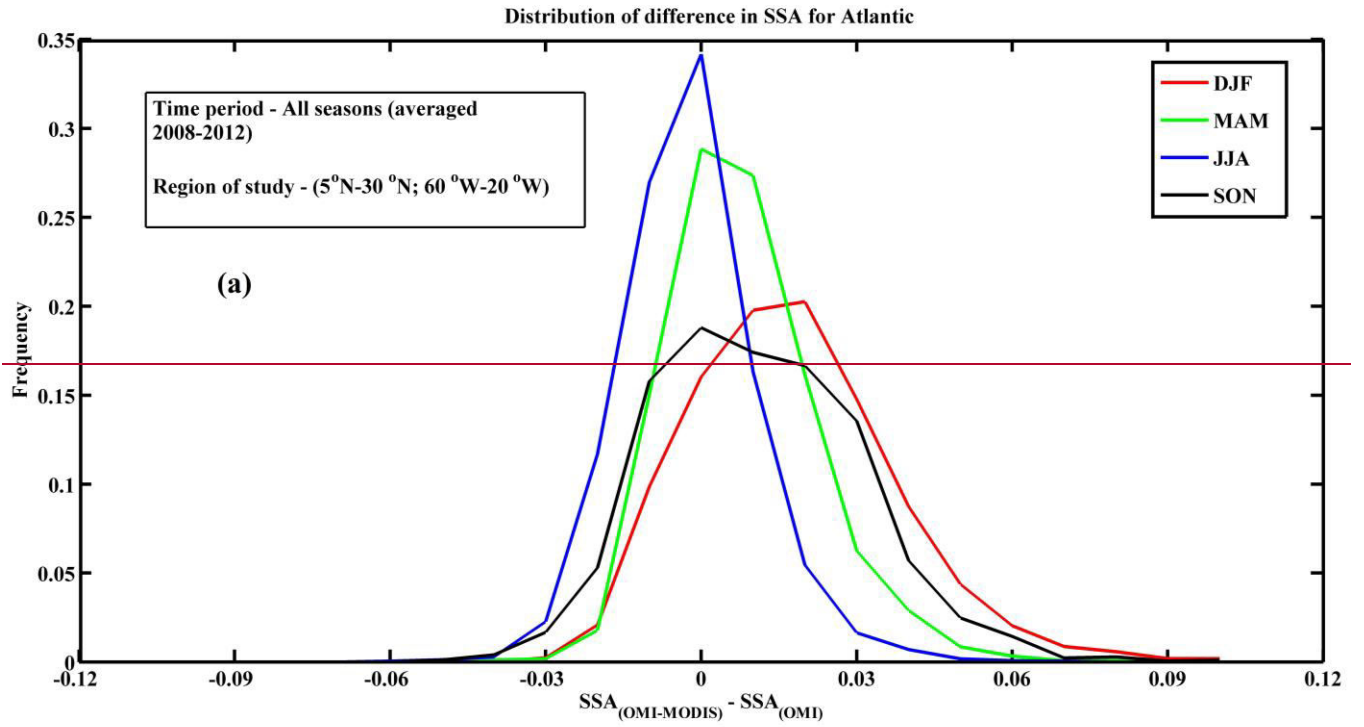


938

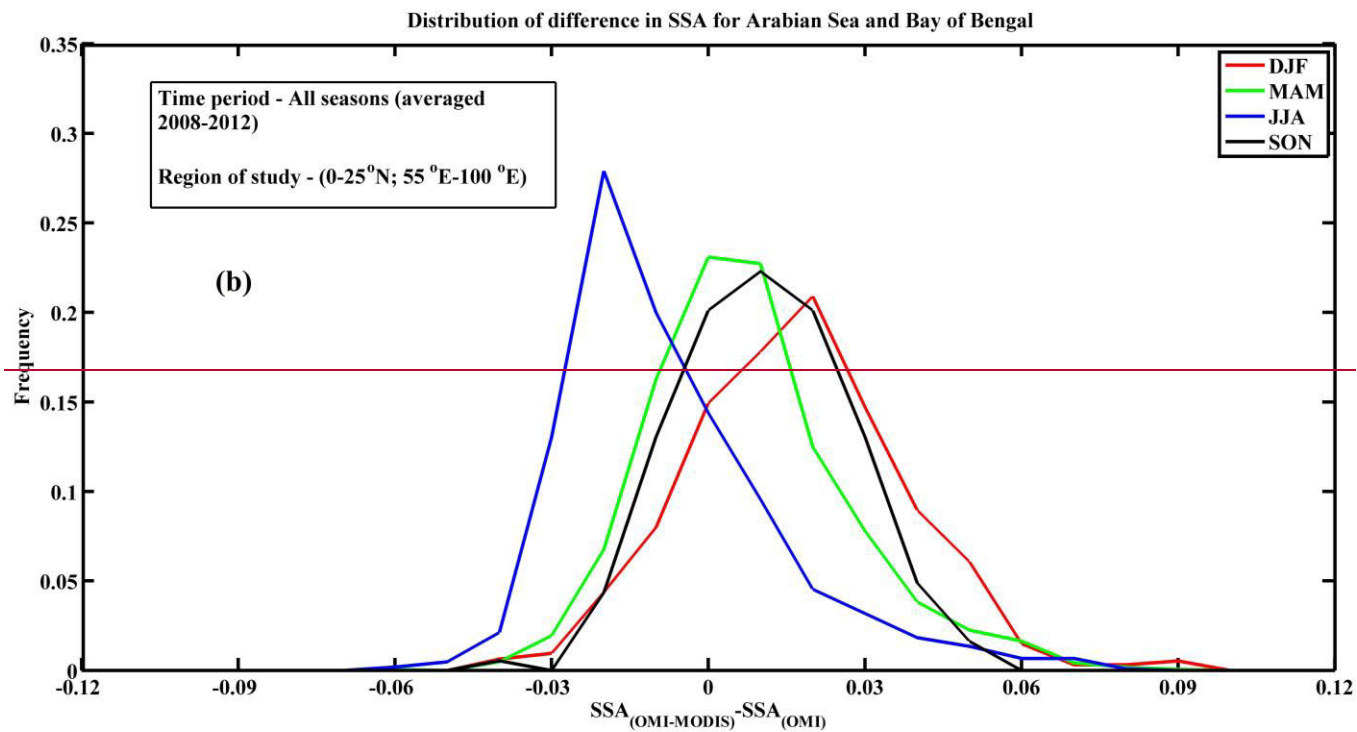
939 **Figure 3.** Distribution of difference in SSA for all seasons averaged over 2008-2012 over a)

940 Atlantic and b) Arabian Sea and Bay of Bengal. [It can be seen that over the Atlantic Ocean, 80%](#)

941 [of the difference in SSA retrievals was within the  \$\pm 0.03\$  range. Over the Arabian Sea and Bay of](#)  
942 [Bengal, the retrievals agreed well during the MAM season when the region was influenced by](#)  
943 [dust.](#)

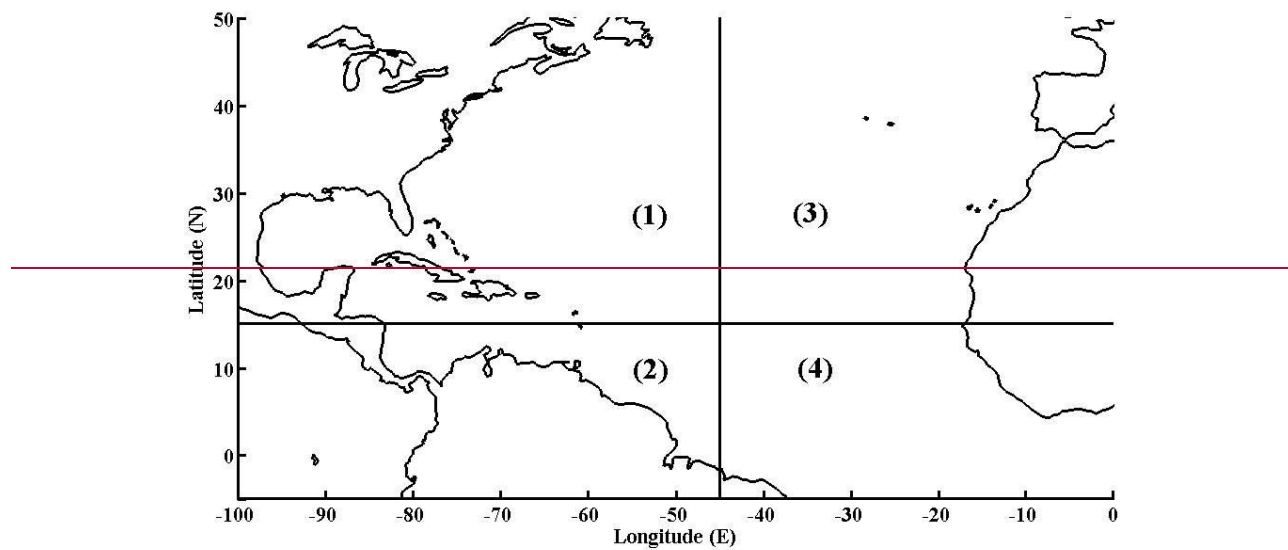


944



945

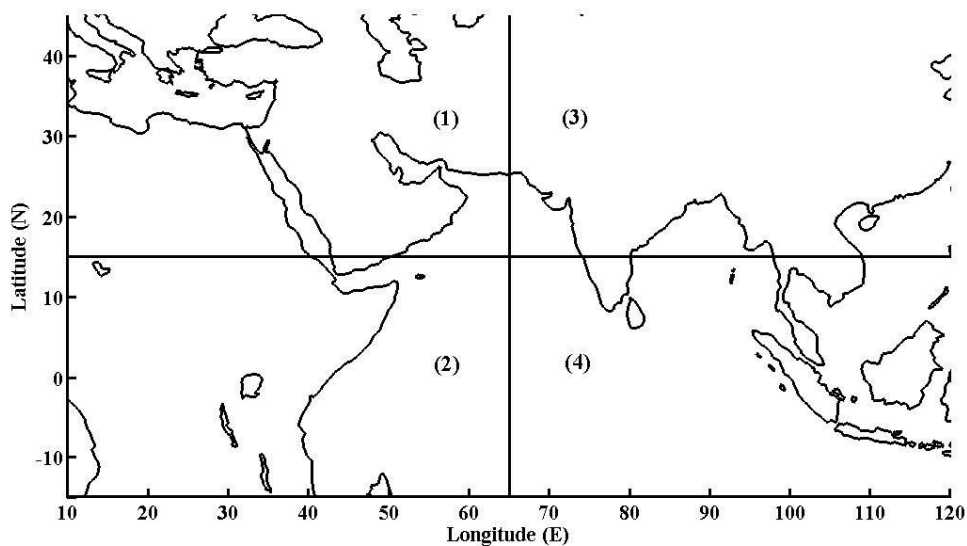
946



947

948 **Figure 4.** Regions representing the various aerosol sources over Atlantic Ocean. 1) North

949 America, 2) Central/South America, 3) North Africa and 4) Southern Africa.

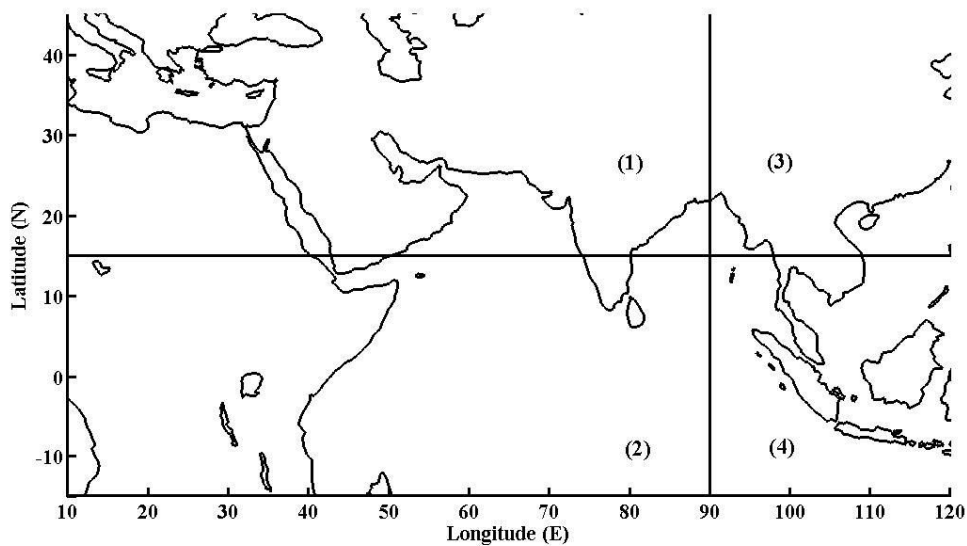


950

951 **Figure 54.** Regions representing the various aerosol sources [for a point](#) over [the](#) Arabian Sea. 1)

952 Arabian Peninsula and North Africa, 2) ~~Southern~~-Central Africa, 3) Indian sub-continent and 4)

953 Indian Ocean and Southeast Asia.



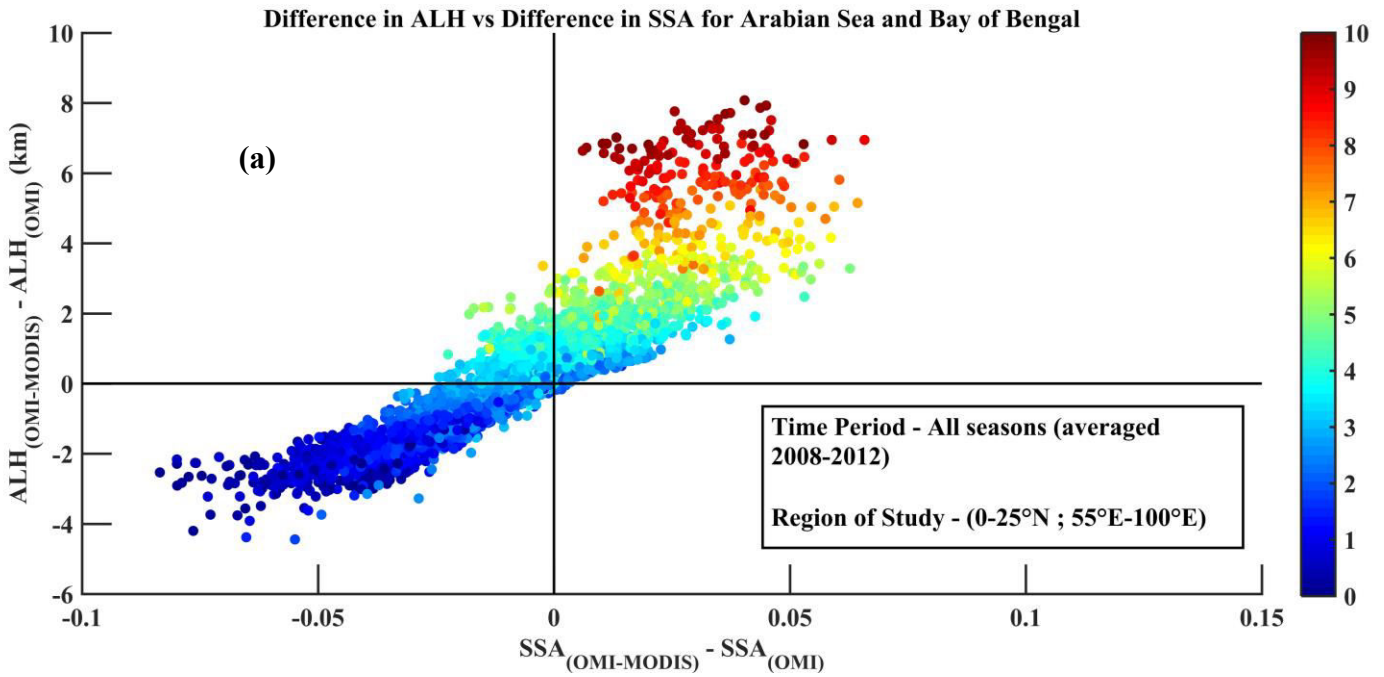
954

955 **Figure 65.** Regions representing the various aerosol sources [for a point](#) over [the](#) Bay of Bengal.

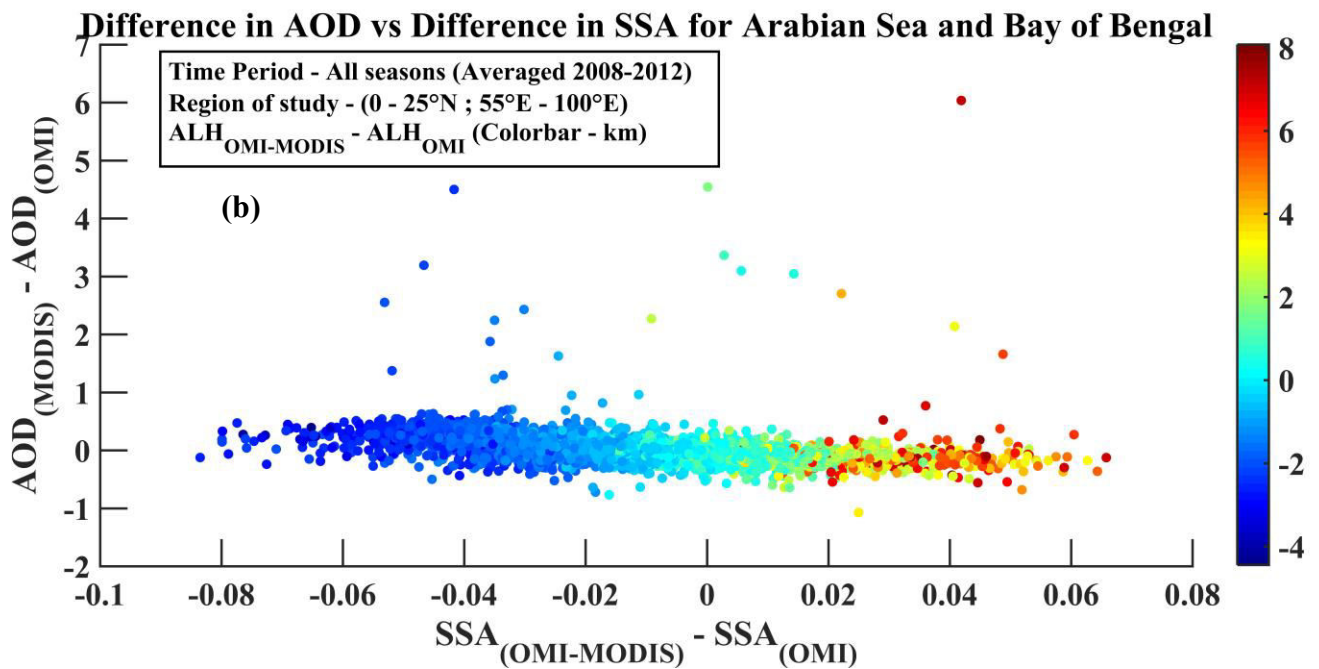
956 1) India/Arabian Peninsula, 2) Indian Ocean, 3) North/Northeast India and East Asia and 4)

957 Southeast Asia.





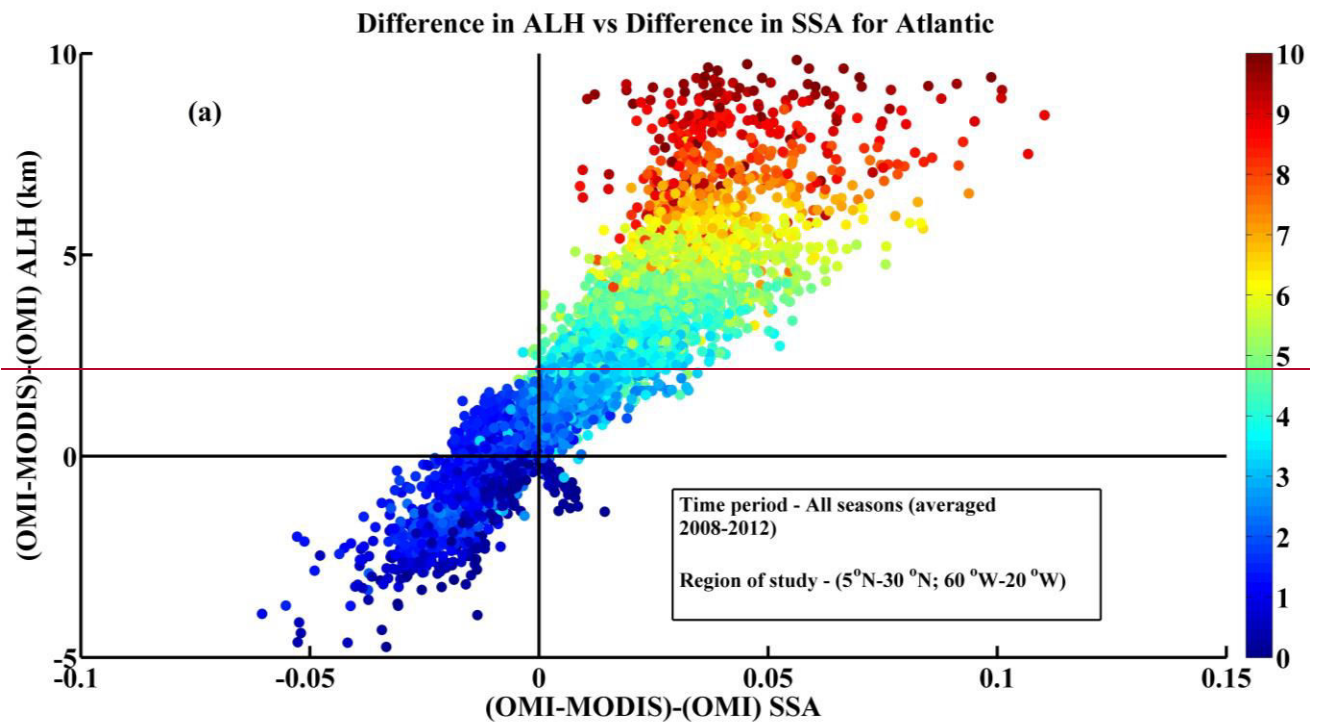
959



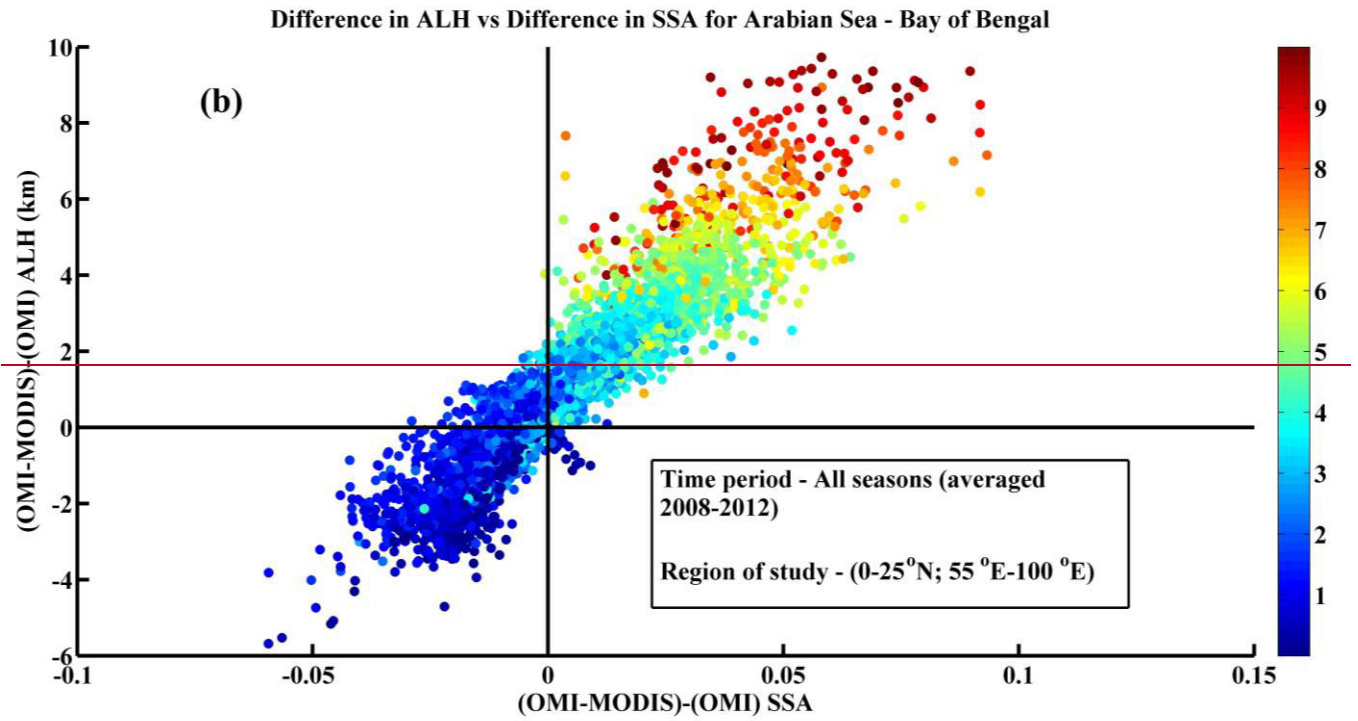
960

961 **Figure 76.** a) Difference in aerosol layer height (ALH - km) between OMI-MODIS and OMI vs.  
 962 difference in SSA over a) ~~Atlantic and b)~~ Arabian Sea and Bay of Bengal. The colorbar  
 963 represents ALH estimated by OMI-MODIS algorithm (km). At lower height (dark blue circles)

964 estimated by OMI-MODIS ~~OMI assumes ALH greater than that of OMI-MODIS and results in~~  
965 ~~overestimation of SSA~~ OMI overestimated SSA when the ALH was overestimated and vice versa  
966 at higher heights estimated by OMI-MODIS b) Difference in AOD ( $AOD_{MODIS} - AOD_{OMI}$ ) has  
967 been plotted with difference in SSA ( $SSA_{OMI-MODIS} - SSA_{OMI}$ ). An inverse relationship was  
968 observed. The colorbar represents the difference in aerosol layer height (ALH - km) between  
969 OMI-MODIS and OMI. -

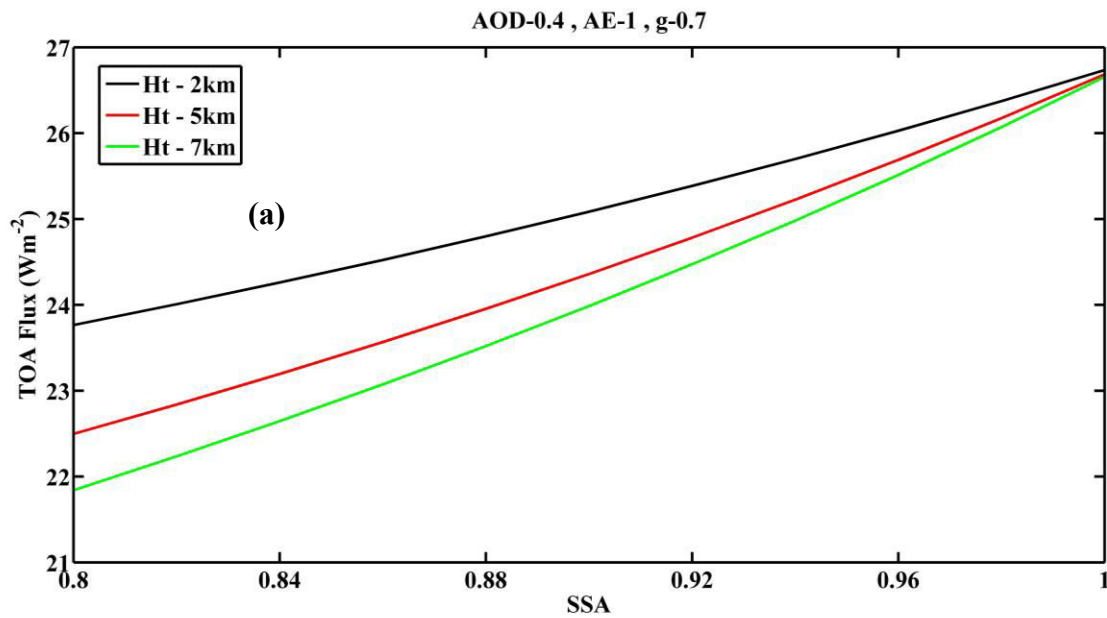


970



971

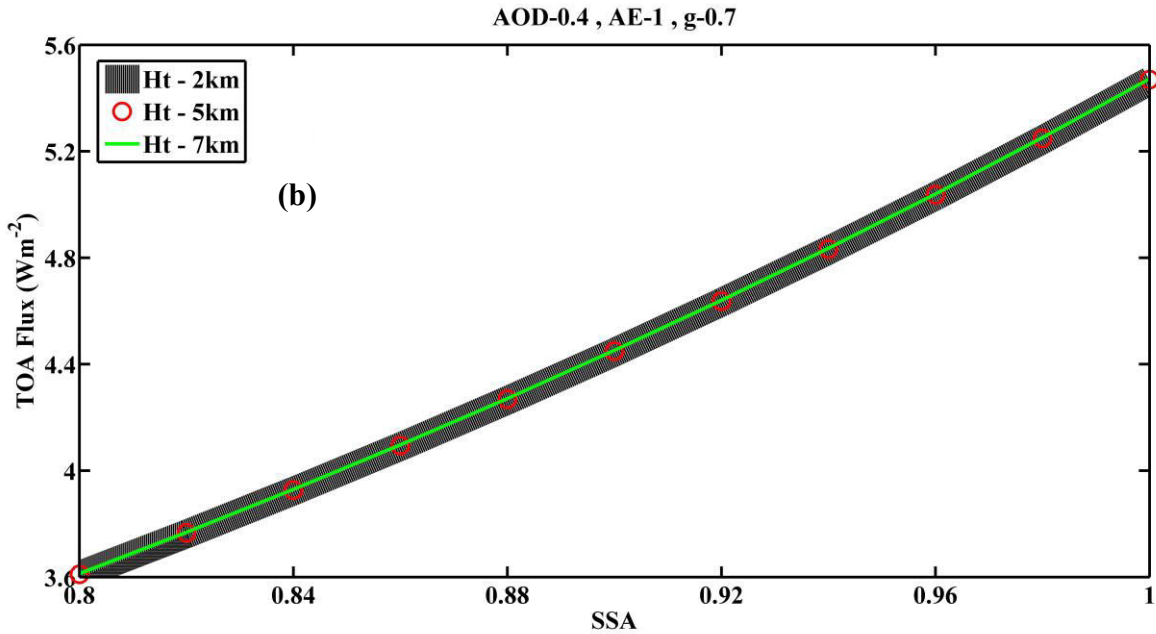
972



973

974

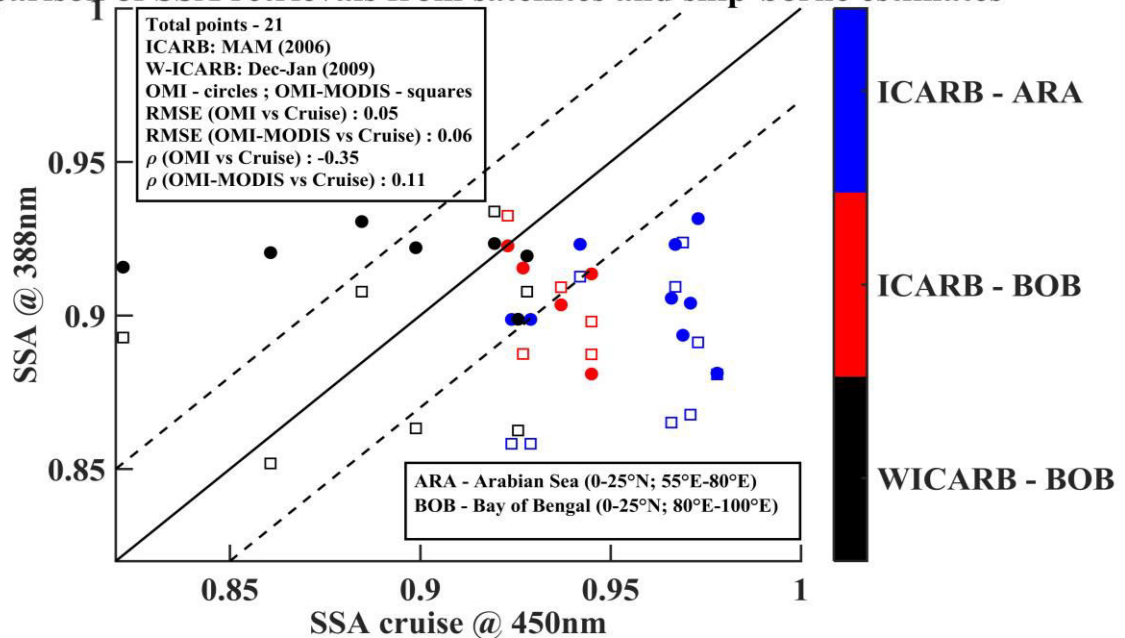
**Figure 8.** TOA flux calculated from SBDART for different SSA and ALH for UV (300-400nm)



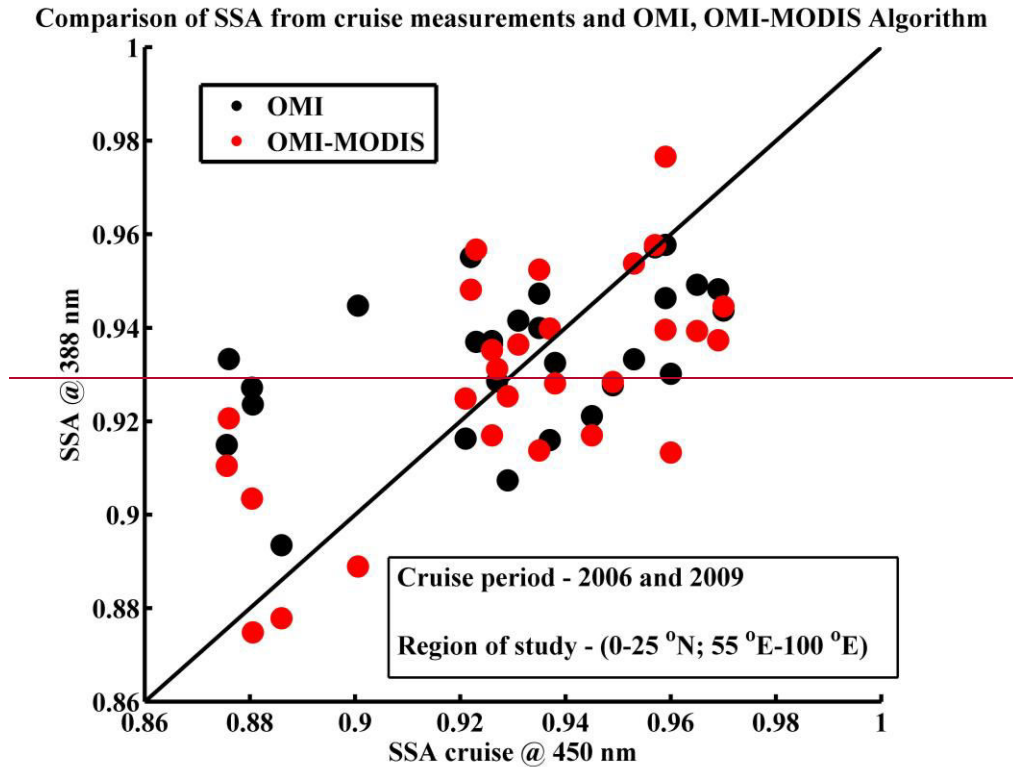
975

976 **Figure 97.** TOA flux calculated from SBDART for different SSA and ALH [a\)](#) with Rayleigh  
 977 scattering [and b\)](#) without Rayleigh scattering removed for UV (300-400nm)

**Comparison of SSA retrievals from satellites and ship-borne estimates**



978



979

980 **Figure 10.** Comparison of  $SSA_{OMI}$  (circles),  $SSA_{OMI-MODIS}$  (squares) with cruise measurements.

981 Each point represents the mean SSA in a 2° box surrounding each cruise location averaged over

982 the respective cruise time period. Due to the sparse nature of OMI-MODIS retrieval, the total

983 number of points common to both the cruise and satellite estimates is only 21. The solid black

984 line is the  $y=x$  line. The dotted lines represent  $\pm 0.03$  range. ~~spatially averaged~~ The colorbar

985 represents the cruise name and the region where the measurements are taken. ICARB (Integrated

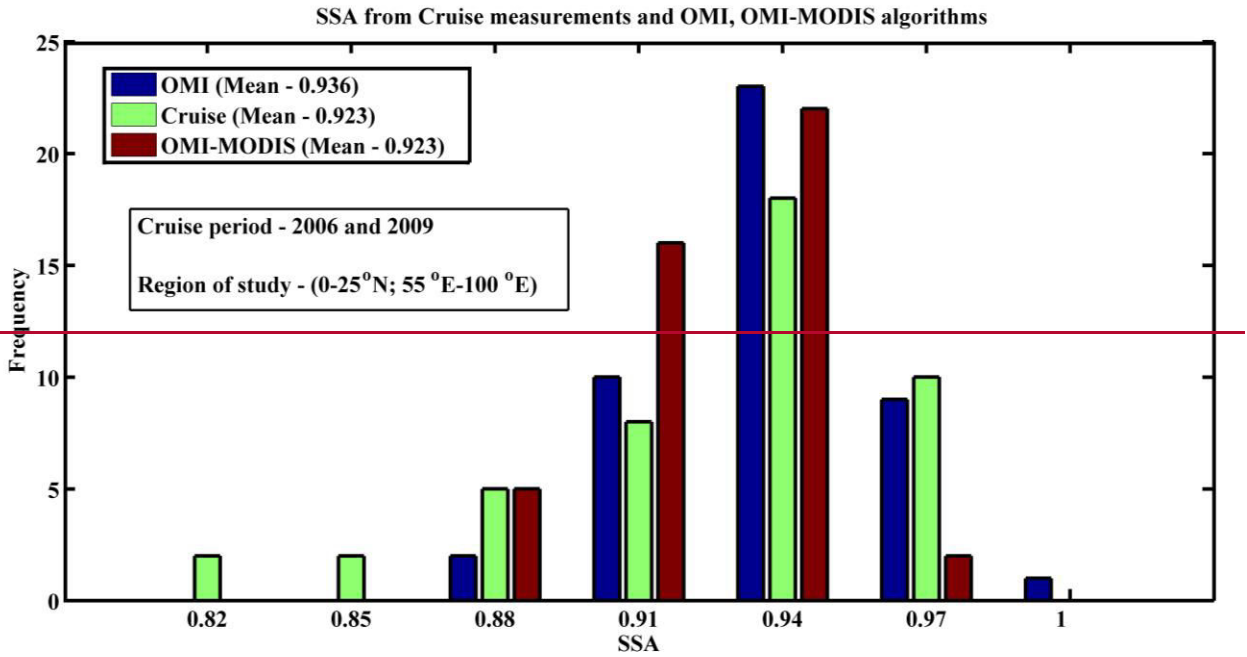
986 Campaign for Aerosols, Gases and Radiation Budget) during March-April-May (MAM) 2006

987 season; W-ICARB (Winter ICARB) during December-January (2008-2009); ARA (Arabian Sea);

988 BOB (Bay of Bengal). Discrepancies between the satellite retrievals and cruise measurements

989 were seen during the ICARB cruise when elevated aerosols were predominantly present over

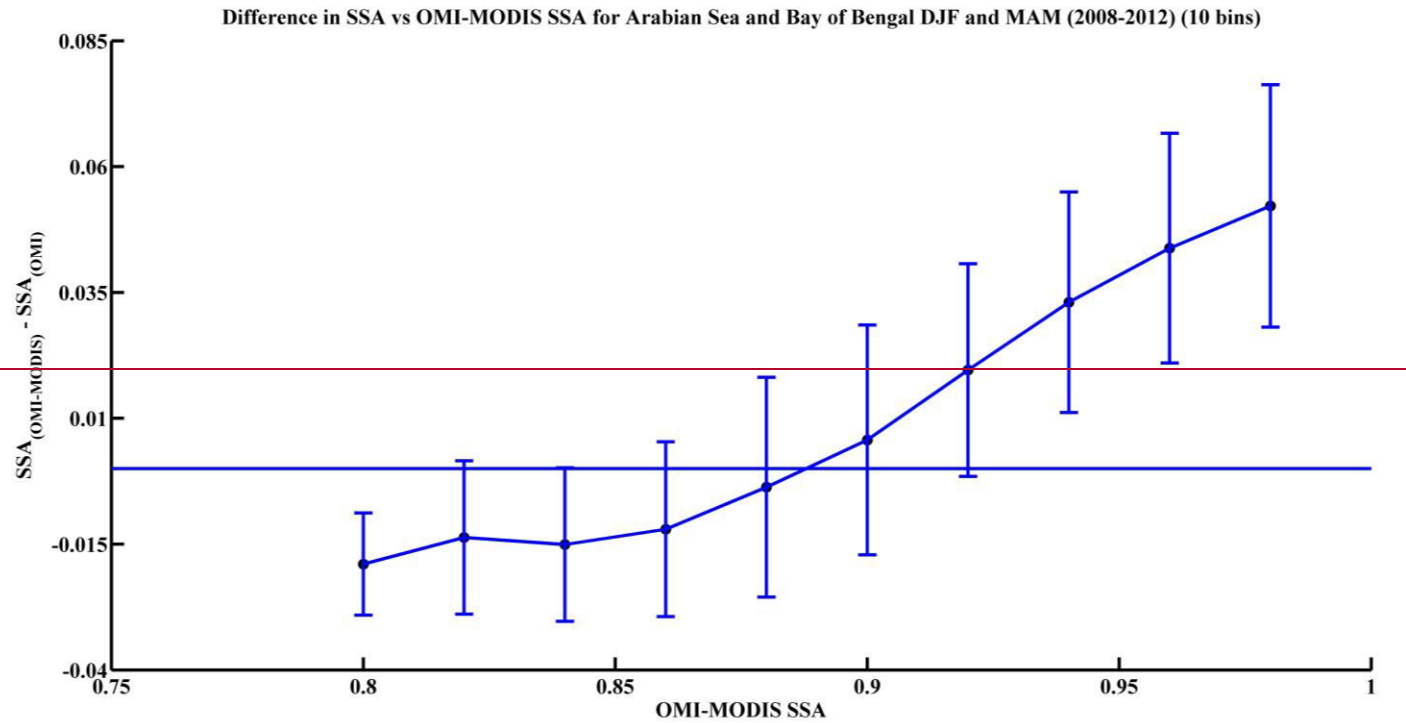
990 both the regions which might not be detected by the cruise measurements.



991

992

**Figure 11.** Distribution of SSA from OMI-MODIS, OMI and cruise measurements.



993

994

995

**Figure 12.** Difference in SSA from OMI-MODIS and OMI Vs SSA from OMI-MODIS. OMI overestimates SSA when absorbing aerosols are detected by OMI-MODIS.

<b>References</b>	<b>Method</b>	<b>Technique</b>	<b>Limitation</b>
Herman et al., 1975; King, 1979; Eck et al., 1998; Dubovik and King, 2000; Torres et al., 2005	Ground-based observations	Inverse methods measurements of solar radiances and/or aerosol properties along with radiative transfer calculations	Measurements are spatially and temporally constrained
Dubovik et al., 2002	Global network – Aerosols Robotic Network (AERONET)	Inverse technique using near-real time measured direct and diffuse radiation	Only land-based, low coverage over remote oceanic regions
Kaufman, 1987; Zhu et al., 2011; Wells et al., 2012	Critical surface reflectance - where the net role of aerosol absorption and scattering becomes independent of aerosol optical thickness and is affected only by SSA	Over varying surface reflectance, the radiance difference between clear and hazy skies is measured using satellite images	Limited spatial variability of surface reflectance. Works only for few cases where there are large amount absorbing aerosols present

Kaufman et al., 2002b	Retrieve SSA in visible wavelengths	Sun-glint is used as a bright background to differentiate role of scattering from aerosol absorption	Only limited scenarios present and does not work on land when absorbing aerosols are present (Torres et al., 2005).
Diner et al., 1998; Remer et al., 2005	Multi Angle Imaging Spectroradiometer (MISR) and Moderate Resolution Imaging Spectroradiometer (MODIS)	Retrieves AOD and SSA in the visible and infrared region of solar spectrum	Surface reflectance influences the retrievals
Herman et al., 1997; Torres et al., 1998	Total Ozone Mapping Spectrometer (TOMS)	Aerosol index parameter is highly sensitive to the Rayleigh scattering thus acting as a bright background in the UV regime	Large pixel size prone to cloud contamination
Torres et al., 2002	Ozone Monitoring Instrument (OMI)	Similar technique as TOMS. Pre-defined aerosol models used.	Sensitive to aerosol layer height and still prone to cloud contamination



996

997 **Table 1.** Ground-based and Satellite-based indirect methods to retrieve SSA

998

<del>Seasons — Regions</del>		<del>1</del>		<del>2</del>		<del>3</del>		<del>4</del>	
		<del>2009</del>	<del>2010</del>	<del>2009</del>	<del>2010</del>	<del>2009</del>	<del>2010</del>	<del>2009</del>	<del>2010</del>
DJF	500m	38%	40%	0%	0%	<b>57%</b>	<b>45%</b>	5%	15%
	1500m	<b>43%</b>	<b>45%</b>	0%	0%	24%	20%	33%	35%
	2500m	<b>52%</b>	<b>50%</b>	10%	10%	5%	15%	33%	25%
MAM	500m	9%	19%	0%	0%	<b>86%</b>	<b>62%</b>	5%	19%
	1500m	<b>33%</b>	<b>38%</b>	0%	4%	<b>53%</b>	<b>29%</b>	14%	29%
	2500m	<b>38%</b>	<b>24%</b>	19%	0%	29%	33%	14%	43%
JJA	500m	5%	5%	0%	0%	<b>90%</b>	<b>90%</b>	5%	5%
	1500m	9%	5%	0%	0%	<b>67%</b>	<b>76%</b>	24%	19%
	2500m	0%	5%	0%	0%	<b>76%</b>	<b>76%</b>	24%	19%
SON	500m	5%	5%	0%	0%	<b>86%</b>	<b>71%</b>	9%	24%
	1500m	0%	10%	0%	0%	<b>81%</b>	<b>71%</b>	19%	19%
	2500m	10%	14%	0%	0%	<b>71%</b>	<b>57%</b>	19%	29%

999

1000 ~~**Table 2.** Influence of various aerosol sources over Atlantic Ocean given as percentage of~~  
 1001 ~~trajectories originating from each source respectively. The maximum influence is given in black~~  
 1002 ~~bold. The different source regions are explained in text and Fig. 4.~~

1003

Seasons \ Regions		1	2	3	4
DJF	500m	<b>57%</b>	0%	38%	5%
	1500m	<b>62%</b>	10%	19%	9%
	2500m	<b>81%</b>	14%	0%	5%
MAM	500m	19%	<b>43%</b>	19%	19%
	1500m	29%	<b>29%</b>	23%	19%
	2500m	<b>57%</b>	14%	24%	5%
JJA	500m	0%	24%	0%	<b>76%</b>
	1500m	19%	<b>67%</b>	0%	14%
	2500m	<b>62%</b>	33%	5%	0%
SON	500m	5%	24%	<b>47%</b>	24%
	1500m	14%	19%	<b>48%</b>	19%
	2500m	<b>38%</b>	10%	19%	33%

1004

1005 **Table 32.** Influence of various aerosol sources over Arabian Sea given as percentage of  
1006 trajectories originating from each source respectively. The maximum influence is given in black  
1007 bold. The different source regions are explained in text and Fig. 54.

1008

Seasons \ Regions		1	2	3	4

DJF	500m	<b>72%</b>	0%	14%	14%
	1500m	<b>48%</b>	14%	10%	28%
	2500m	29%	33%	0%	<b>38%</b>
MAM	500m	19%	<b>48%</b>	0%	33%
	1500m	<b>57%</b>	29%	20%	14%
	2500m	<b>71%</b>	24%	0%	5%
JJA	500m	0%	<b>100%</b>	0%	0%
	1500m	5%	<b>95%</b>	0%	0%
	2500m	14%	<b>81%</b>	0%	5%
SON	500m	5%	<b>52%</b>	33%	10%
	1500m	5%	<b>43%</b>	<b>43%</b>	9%
	2500m	5%	<b>33%</b>	29%	<b>33%</b>

1009

1010 **Table 43.** Influence of various aerosol sources over Bay of Bengal given as percentage of  
1011 trajectories originating from each source respectively. The maximum influence is given in black  
1012 bold. The different source regions are explained in text and Fig. 65.

	<b>OMI</b>	<b>OMI-MODIS</b>
<del>Mean SSA (Cruise—0.923)</del>	<del>0.936</del>	<del>0.923</del>
<del>Std. Dev. (Cruise—0.04)</del>	<del>0.021</del>	<del>0.021</del>
<del>p-value</del>	<del>0.046</del>	<del>0.981</del>
<del>Confidence Interval</del>	<del>[0.0002, 0.027]</del>	<del>[-0.013, 0.013]</del>

1013

1014 **Table 5.** Comparison of SSA between both the satellite algorithms and cruise measurement